2018

Stability of periodic orbits in no-slip billiards

C. Cox
Tarleton State University

R. Feres
Washington University in St. Louis

Hongkun Zhang
University of Massachusetts Amherst

Recommended Citation
Cox, C.; Feres, R.; and Zhang, Hongkun, "Stability of periodic orbits in no-slip billiards" (2018). *Nonlinearity*. 1290.
https://doi.org/10.1088/1361-6544/aacc43

PAPER

Stability of periodic orbits in no-slip billiards

IOP Publishing | London Mathematical Society Nonlinearity

Nonlinearity **31** (2018) 4443–4471 https://doi.org/10.1088/1361-6544/aacc43

Stability of periodic orbits in no-slip billiards

C Cox[1], R Feres[2] and H-K Zhang[3]

[1] Department of Mathematics, Tarleton State University, Box T-0470, Stephenville, TX 76402, United States of America
[2] Department of Mathematics, Washington University, Campus Box 1146, St. Louis, MO 63130, United States of America
[3] Department of Math. & Stat., University of Massachusetts Amherst, MA 01003, United States of America

E-mail: feres@wustl.edu

Received 11 December 2016, revised 8 June 2018
Accepted for publication 13 June 2018
Published 21 August 2018

Recommended by Professor Konstantin M Khanin

Abstract

Rigid bodies collision maps in dimension-two, under a natural set of physical requirements, can be classified into two types: the standard specular reflection map and a second which we call, after Broomhead and Gutkin, *no-slip*. This leads to the study of *no-slip billiards*—planar billiard systems in which the moving particle is a disc (with rotationally symmetric mass distribution) whose translational and rotational velocities can both change after collisions with the boundary of the billiard domain.

This paper, which continues the investigation initiated in Cox and Feres (2017 *Dynamical Systems, Ergodic Theory, and Probability: in Memory of Chernov* (Providence, RI: American Mathematical Society), is mainly focused on the issue of stability of periodic orbits in no-slip planar billiards. We prove Lyapunov stability of periodic orbits in polygonal billiards of this kind and, for general billiards domains, we obtain curvature thresholds for linear stability at commonly occurring period-2 orbits. More specifically, we prove that: (i) for billiard domains in the plane having piecewise smooth boundary and at least one corner of inner angle less than π, no-slip billiard maps admit elliptic period-2 orbits; (ii) polygonal no-slip billiards under this same corner angle condition always contain small invariant neighborhoods of the periodic point on which, up to smooth conjugacy, orbits of the return map lie on concentric circles; in particular the system cannot be ergodic with respect to the canonical invariant billiard measure; (iii) the no-slip version of the Sinai billiard must contain linearly stable periodic orbits of period 2 and, more generally, we obtain a curvature threshold at which the period-2 orbits go from being hyperbolic

to being elliptic; (iv) finally, we make a number of observations concerning periodic orbits in wedge and triangular billiards. Our linear stability results extend those of Wojtkowski for the no-slip Sinai billiard.

Keywords: no-slip billiards, rigid body collisions, orbit stability and chaos
Mathematics Subject Classification numbers: Primary: 37J99, Secondary: 53Z05

(Some figures may appear in colour only in the online journal)

1. Introduction

Consider a billiard dynamical system consisting of a planar domain, referred to as the *billiard table*, and a small disc with rotationally symmetric mass distribution, the *billiard particle*, that slides and rotates freely between successive collisions with the boundary of the table. Upon collision, the particle reflects according to standard mechanics textbook assumptions for conservative rigid body impact to be spelled out shortly. It has long been known that the linear map giving the angular and center of mass velocities immediately after impact in terms of the velocities immediately prior is not uniquely determined; there are exactly two possibilities, each corresponding to a different assumption about the nature of the disc-boundary contact. One possibility represents a perfectly slippery contact that does not create any coupling between translational and angular motion. In this case, by following the center of mass and ignoring rotation, the system reduces to the ordinary two-dimensional billiard motion of a point particle with specular reflection to which most of the literature concerning billiard dynamics is dedicated.

The second possibility represents a perfectly non-slippery contact. This corresponds to a sort of non-dissipative static friction that allows for linear and angular momentum to be partially exchanged at collision. We refer to this type of contact and associated billiards as *no-slip*. They generate a four-dimensional dynamical system (that is to say, the system is generated by the iterations of a map on a four-dimensional energy hypersurface of the billiard phase space) having a number of very distinct properties that are in sharp contrast with ordinary billiard dynamics in two (or higher) dimensions.

One striking difference has to do with stability of periodic orbits—the main topic of concern of the present paper. A ubiquitous feature of no-slip billiards in dimension-two, which is clearly apparent from numerical simulation, is the presence of elliptic islands near periodic points. These islands exist amid chaos created, apparently, by the usual mechanisms of dispersing and focusing. It is also apparent that this elliptic behavior is very hard to destroy, as the no-slip counterpart to the Sinai billiard will illustrate. The picture that emerges in this study suggests that finding ergodic examples of no-slip billiards—one of our initial motivations—is a challenging problem. We note, in passing, that the no-slip billiard map is not symplectic, although it retains some features of symplectic maps. (See section 5 on measure invariance and reversibility.) On the other hand, the billiard map does preserve the standard Liouville measure and it is time-reversible. The proposed problem of finding ergodic no-slip billiards is for this natural invariant measure.

The no-slip interaction is, naturally (given the above mentioned classification, stated formally in proposition 3), used whenever rotational effects become important. For example, in [7, 9] the authors apply it to models of transport phenomena in Statistical Mechanics. And

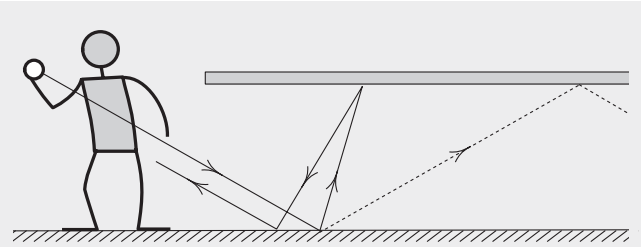

Figure 1. Rendering of Richard L. Garwin's illustration in his 1969 paper *Kinematics of an Ultraelastic Rough Ball,* in which he introduces the no-slip condition to model the bouncing of a Wham-O Super Ball®.

in [5], by Garwin, published in the American Journal of Physics in 1969, the author introduces the no-slip condition to explain how a *super ball* can return to the hand after bouncing against the underside of a table (our figure 1 reproduces with less charm figure 1 of his paper). However, very little has been done, to the best of our knowledge, to systematically develop the dynamics and ergodic theory of no-slip planar billiards. Aside from our [3, 4], we know of research by Broomhead and Gutkin [1] showing that no-slip billiard orbits in an infinite strip are bounded; and by Wojtkowski [12], characterizing linear stability for a special type of period-2 orbit. Here we extend the main result of [1] (on the boundedness of orbits of no-slip billiards on an infinite strip) to wedges, from which our stability result for general polygonal billiards is derived; and we extend the linear stability result of [12] to more general types of periodic orbits.

The following theorems contain the main results of the present paper.

Theorem 1. *Let us consider a polygonal billiard domain, not necessarily bounded, having at least one corner with inner angle less than π. Then the no-slip billiard map admits periodic orbits of period 2. Periodic orbits (of any period), moreover, are Lyapunov stable. That is, given an initial state ξ for a period-n orbit and any neighborhood $\mathcal{V}$ of ξ, there exists a small enough neighborhood $\mathcal{U} \subset \mathcal{V}$ of ξ such that orbits of elements in $\mathcal{U}$ remain in $\mathcal{V}$. It follows that the canonical billiard measure (also known as the Liouville measure, which is invariant under the no-slip billiard map), is never ergodic for such polygonal billiards.*

As will be seen, period-2 orbits are very common in, not necessarily polygonal, no-slip billiards, although extending the above theorem in the presence of curvature appears presently to be a challenging problem. Nevertheless, we show that (linearly) elliptic periodic orbits exist under very general conditions. The next result gives a sufficient condition for that.

Theorem 2. *Suppose that the billiard domain of the no-slip billiard system has a piecewise smooth boundary with at least one corner with inner angle less than π. Then, arbitrarily near such a corner one finds (linearly) elliptic period-2 orbits.*

We stress that local (Lyapunov) stability is not shown here unless the boundary curvature is zero in a neighborhood of the periodic orbit. It should be recalled in this regard that, different from the dimension-two case in which, by a result of Moser [8], a generic elliptic fixed point of an area-preserving map is Lyapunov stable, the same is not true in dimension-four even for symplectic maps, as shown in [6]. Our Lyapunov stability result of the above first theorem depends on an explicit normal-form construction that works so far in zero curvature. It is possible that special features of the no-slip billiard maps together with KAM-type results for reversible systems such as proved in [10] can be used to obtain a stronger result, but we

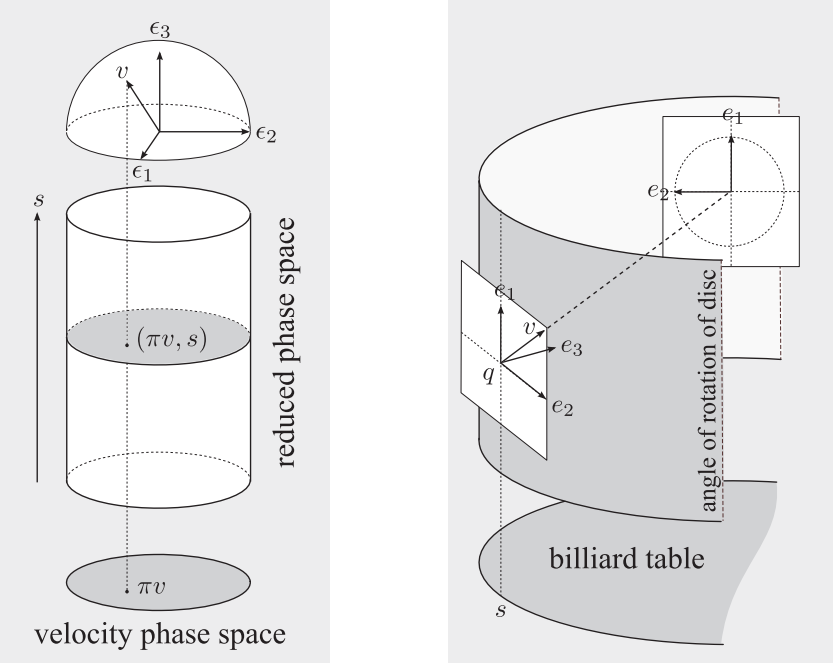

Figure 2. Several definitions from this section are illustrated here. The no-slip billiard map acts on three-dimensional vectors v encoding the linear and angular velocities of the particle immediately after a collision with $\partial\mathscr{B}$. The positive orthonormal basis (e_1, e_2, e_3) of T_qM, where e_3 is the unit normal vector to ∂M pointing into M and e_2 is tangent to $\partial\mathscr{B}$ at q, is called here the *product frame* at q. The same symbol v is used for the vector $(v \cdot e_1)\epsilon_1 + (v \cdot e_2)\epsilon_2 + (v \cdot e_3)\epsilon_3$ where $(\epsilon_1, \epsilon_2, \epsilon_3)$ is the standard basis in $\mathbb{R}^3$. The unit disc in the plane spanned by ϵ_1 and ϵ_2 is the *velocity phase space*. Points in it represent the orthogonal projection to $T_q(\partial M)$ of post-collision velocities. Here s indicates the arc-length parameter of $\partial\mathscr{B}$. The Cartesian product of the velocity phase space and the interval range of s is the *reduced phase space*, indicated here as the solid vertical cylinder on the left. Notice that the s-axis on the left maps to the boundary of the billiard table on the right-hand side of the figure.

do not resolve this issue here. What we do obtain for the non-flat case are sharp curvature threshold values at which the periodic orbits transition from (linearly) hyperbolic to elliptic, generalizing the main result of [12]. The above theorem 2 is a consequence of these observations. (See section 8.)

A few remarks are in order concerning notation and visualization. As we are dealing with a four-dimensional system, usefully visualizing the dynamics is less straightforward than it is for the familiar (slip) planar billiards. By a natural projection, essential features can be described in dimension-three, in what we refer to as the *reduced phase space*, depicted on the left part of figure 2. (This will be explained shortly.) The cylinder's cross-sectional disc at height s is the 'flattened out' hemisphere of (outgoing) translational-angular velocities of the billiard particle (which are unit vectors in the kinetic energy norm) after colliding with the point on the boundary of the billiard table having arc-length parameter value s. In our computer illustrations, we have found it often illuminating to present not the (reduced, three-dimensional) system's phase portrait but the two-dimensional projections exemplified in figure 3. On the left part of figure 3 is the trajectory of the center of mass of the moving disc (the billiard table is suitably shrunk at the margin by the radius of the particle), and on the right is

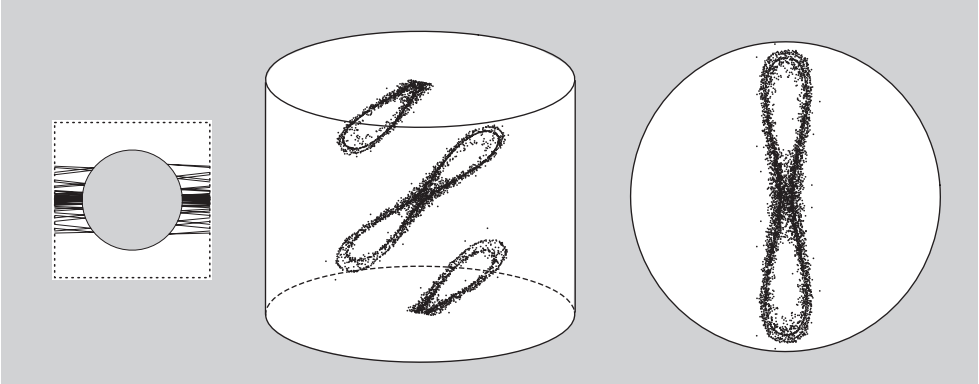

Figure 3. Illustration of the concept of *reduced* and *velocity phase space*. Here the system is the no-slip Sinai billiard studied in section 9. On the left we see the projection of an orbit segment to the plane of $\mathscr{B}$. In the middle is the same orbit shown in the reduced phase space (this is the same cylinder shown on the left-hand side of figure 2) and, on the right, is the velocity phase space. The latter is the projection of the orbit along the axis of the cylinder.

the projection of an orbit from the solid cylinder to its circular base. The latter projection will be referred to as a *velocity phase portrait*. Velocity portraits thus depict not a single slice of the cylinder (that is, the three-dimensional reduced phase space) but its entire projection. This means that a feature of the orbits revealed in the velocity phase portrait reflects what goes on in all slices. (We refer the reader to our [4] for many illustrations of velocity portraits for a variety of billiard shapes.)

Concerning notation, a compromise had to be reached between writing linear maps in matrix form in a fixed basis, yielding simpler but maybe more opaque notation, or using a more conceptual, coordinate-free description that imposes greater typographical burden but is much more compact to write. (This is particularly the case in sections 4 and 5.) Readers familiar with standard billiard notation such as used in [2] may not approve of our choice to lean towards the latter, but we believe the alternative would have made the paper longer and more difficult to follow.

The paper is organized as follows. Section 2 introduces the main notations and definitions; section 3 gives the general description of period-2 orbits; section 4 expresses the differential of the no-slip billiard map in convenient form for use in the succeeding sections; section 5 proves invariance of the standard (Liouville) billiard measure and derives a useful consequence from time reversibility of the billiard map; section 6, which is the technical core of the paper, contains the main stability result for wedge billiards and period-2 orbits and relies on the results of all the previous sections; section 7 extends the main result of the previous section to periodic orbits of general period and gives a classification of periodic orbits on the wedge; section 8 derives curvature conditions for period-2 orbits to be elliptic; section 9 illustrates the curvature threshold separating hyperbolic and elliptic behavior for periodic orbits of the non-slip version of the Sinai billiard (positive boundary curvature) and, more briefly, for a family of domains with negative boundary curvature. The brief final section 10 gives a rough conjectural picture of what non-slip billiard dynamics on bounded polygons should look like based on numerical experiments.

This paper has been much improved by the many recommendations of an anonymous referee, to whom the authors wish to express their sincere gratitude.

2. Definitions and basic facts

Let $\mathscr{B} \subset \mathbb{R}^2$ be a connected region having piecewise smooth boundary, to be referred to as the *billiard table*. Let D denote the disc of radius R in $\mathbb{R}^2$ centered at the origin and μ a finite measure on D representing mass distribution with total mass $m := \mu(D)$ whose center of mass coincides with the center of D at 0. We write the moment of inertia of μ as $\mathscr{I} = m(\gamma R)^2$. For the uniform mass distribution, for example, the parameter γ defined by this expression is $\gamma = 1/\sqrt{2}$, and in general $0 \leqslant \gamma \leqslant 1$. It is also useful to define $\beta > 0$ such that $\gamma = \tan^2(\beta/2)$. The quantities

$$\cos\beta = \frac{1-\gamma^2}{1+\gamma^2}, \quad \sin\beta = \frac{2\gamma}{1+\gamma^2}$$

will be used throughout the paper.

By a *configuration* of the *billiard particle* D we mean the Euclidean transformation that rotates D by an angle θ and translates the result by an element in $\mathscr{B}$. It will be convenient to introduce the rotation coordinate $x := \gamma R\theta$. It parametrizes a point (also denoted by x) on the 1-torus $\mathbb{T} := \mathbb{R}/(2\pi\gamma R)$. The three-dimensional configuration manifold of the billiard system is then $M := \mathscr{B} \times \mathbb{T}$. Points in M will be written as $q = (\bar{q}, x)$. With our choice of x, the kinetic energy of a state (q, v) in the tangent bundle TM is simply $\frac{1}{2}m|v|^2$, where $|v|$ is ordinary Euclidean norm in $\mathbb{R}^3$.

Figure 2 illustrates the definition of the (e_1, e_2, e_3)-frame. We focus for now on the right-hand side of that figure. It depicts part of the three-dimensional configuration manifold M and its projection to the billiard table $\mathscr{B}$. On each $q \in \partial M$ we define $e_1 = (0,0,1)$, $e_2(q)$ the unit vector tangent to $\partial\mathscr{B}$ at q pointing counterclockwise when viewing $\mathscr{B}$ from above (where 'up' is set by e_1) and $e_3(q)$ the unit vector perpendicular to $T_q(\partial M)$ pointing into M. These are unit vectors in the standard Euclidean metric, which is proportional to the Kinetic energy metric (the constant of proportionality is the mass m).

The *phase space* of the billiard system will be defined as

$$N := N^+ := \{(q, v) \in T\mathbb{R}^3 : q \in \partial M, |v| = 1, v \cdot e_3(q) > 0\}.$$

Elements of N are the *post-collision velocities* and elements of N^-: $= -N$ are the *pre-collision velocities*. The vector space fiber of $N^\pm$ at q will be denoted $N_q^\pm$. Thus $v \in N_q^\pm$ if $(q, v) \in N^\pm$. The projection of v to $T_{\bar{q}}\mathscr{B}$ is the center of mass velocity and $v \cdot e_1$ is proportional to angular velocity.

By a *collision map* at $q \in \partial M$ we mean a linear map $C_q : T_qM \to T_qM$ sending N_q^- into N_q. Proposition 3 contains a very special case of the main result of [3], which classifies collision maps for collisions of rigid bodies in $\mathbb{R}^n$ under the following assumptions: energy, translation and angular momenta are conserved, the process is time reversible, and impulse forces between the bodies can only act at the single point of contact. For billiard systems, where one of the bodies (the billiard table) is fixed in place, momentum conservation is typically void as the group of Euclidean symmetries of the system may be trivial. The last assumption is very strong and, in fact, it generalizes momentum conservation in a sense that is explained in [3].

The following subspaces tangent to $\partial M = \partial\mathscr{B} \times \mathbb{T}$ are needed in the definition of the no-slip collision map. Let $q \in \partial M$ and define

$$\mathfrak{S}_q = \{a(-\gamma e_1 + e_2(q)) : a \in \mathbb{R}\}, \quad \overline{\mathfrak{C}}_q = \{a(e_1 + \gamma e_2(q)) : a \in \mathbb{R}\}.$$

Then $\mathfrak{S}_q$ and $\overline{\mathfrak{C}}_q$ are orthogonal subspaces of $T_q(\partial M)$.

Proposition 3. *Under the assumptions of energy conservation, time reversibility, and that impulse forces can only act at the point of contact, the collision map C_q sends $e_3(q)$ to its negative, the restriction of C_q to $\mathfrak{S}_q$ is the identity, and its restriction to $\overline{\mathfrak{C}}_q$ is either plus or minus the identity. The plus sign gives the standard specular reflection map, and the minus sign gives the no-slip map.*

On account of this proposition, the standard (slip) and the no-slip billiard reflections seem to have an equal standing as mathematical models of particle collision. As will be noted shortly, however, the system corresponding to the no-slip collision is not Hamiltonian. We speculate that a Hamiltonian model of Garwin's superball behavior would require taking into account more degrees of freedom than a rigid body can have.

For each boundary configuration q let $\sigma_q : \mathbb{R}^3 \to T_q\mathbb{R}^3$ be the orthogonal map sending the standard basis vectors ϵ_i of $\mathbb{R}^3$ to $e_i(q)$. Then C_q is represented in the frame (e_1, e_2, e_3) at any q by

$$\mathscr{C} = \sigma_q^{-1} C_q \sigma_q = \begin{pmatrix} -\cos\beta & -\sin\beta & 0 \\ -\sin\beta & \cos\beta & 0 \\ 0 & 0 & -1 \end{pmatrix}. \tag{1}$$

Definition 4 (The no-slip billiard map). The no-slip billiard map T is the composition of the free motion between two points q_1, q_2 in ∂M and the no-slip collison map C_{q_2} at the endpoint. Thus $T : N \to N$ is given by $(\tilde{q}, \tilde{v}) = T(q, v) = (q + tv, C_{\tilde{q}} v)$ where $t := \inf\{s > 0 : q + sv \in N\}$.

Although the notation $T : N \to N$ suggests that T is defined on all of N, as with ordinary billiard maps its domain should exclude a set of singular points. Here we assume that the shape of the billiard table $\mathscr{B}$ is such that T makes sense and is smooth for all ξ in some big subset of N, say open of full Lebesgue measure. This condition will hold for all the billiard domains considered in this paper.

Now let

$$\xi = (q, v) \mapsto \tilde{\xi}_- = (\tilde{q}, v) \mapsto \tilde{\xi} = \tilde{\xi}_+ = (\tilde{q}, C_{\tilde{q}} v).$$

The first map in this composition is parallel translation of v from q to $\tilde{q}$; it will be denoted by Φ. The second map, C, applies the no-slip reflection to the translated vector, still denoted v, at $\tilde{q}$. Hence $T = C \circ \Phi$.

Taking into account the rotation symmetry of the moving disc, we may for most purposes ignore the angular coordinate (but not the angular velocity!) and restrict attention to the *reduced phase space*. This is defined as $\partial\mathscr{B} \times \{u \in \mathbb{R}^2 : |u| < 1\}$, where an element u of the unit disc represents the velocity vector at $q \in \partial\mathscr{B}$ (pointing into the billiard region) given by

$$\sigma_q\left(u_1, u_2, \sqrt{1 - |u|^2}\right) = u_1 e_1(q) + u_2 e_2(q) + \sqrt{1 - |u|^2} e_3(q).$$

By *velocity phase space* we mean this unit disc. The left-hand side of figure 2 summarizes these definitions.

As an example of the reduced and velocity phase spaces we point to figure 3. It shows what an orbit segment looks like in these spaces for the no-slip Sinai billiard. The domain $\mathscr{B}$ for this system is defined as the complement of a disc in the 2-torus. The Sinai billiard will be used throughout the paper to illustrate various concepts and results. We refer to [12] for further information and motivation. The reader should bear in mind that, when we represent billiard orbits as on the left of figure 3 (or, for example, in figure 9), we are only showing

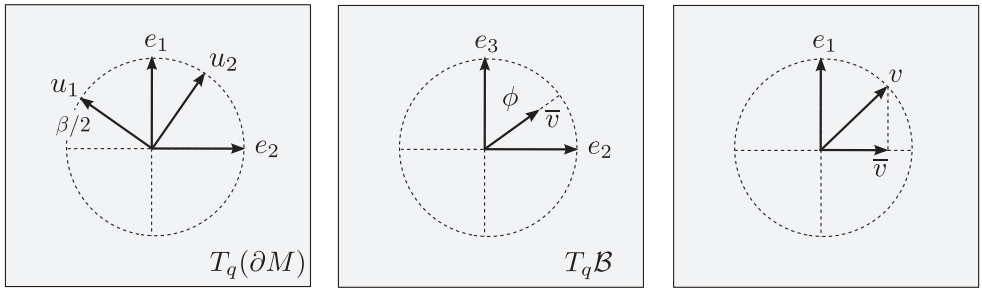

Figure 4. Frame definitions: the q-dependent product frame $(e_i(q))$, the eigenframe $(u_i(q))$ for the collision map C_q at a collision configuration $q \in \partial M$; β is the characteristic angle of the system (a function of the mass distribution of the disc). The angle φ is defined by this figure.

the projections on the plane of the billiard table $\mathscr{B}$; the angle of rotation axis is typically not shown. (Figure 6 is an exception.)

The rotation symmetry that justifies passing from the four-dimensional phase space to the three-dimensional reduced phase space may be formally expressed by the identity

$$T(q + \lambda e_1, v) = T(q, v) + \lambda e_1.$$

Note that e_1 is independent of q and that $\mathrm{d}T_\xi e_1 = e_1$ for all $\xi = (q, v)$, where $\mathrm{d}T_\xi$ is the differential map of T at ξ.

In addition to $(e_1(q), e_2(q), e_3(q))$ (equivalently, σ_q) it will be useful to introduce a frame consisting of eigenvectors of the collision map C_q. We define

$$\begin{aligned} u_1(q) &= \sin(\beta/2)e_1(q) - \cos(\beta/2)e_2(q) \\ u_2(q) &= \cos(\beta/2)e_1(q) + \sin(\beta/2)e_2(q) \\ u_3(q) &= e_3(q). \end{aligned} \tag{2}$$

See figure 4. Then

$$C_q u_1(q) = u_1(q), \;\; C_q u_2(q) = -u_2(q), \;\; C_q u_3(q) = -u_3(q).$$

Yet a third orthonormal frame will later prove useful in our analysis of period-2 orbits. Let $\xi = (q, v) \in N$. Then $w_1(\xi), w_2(\xi), w_3(\xi)$ is the orthonormal frame at q such that

$$w_1(\xi) := \frac{e_1(q) - e_1(q) \cdot vv}{|e_1(q) - e_1(q) \cdot vv|}, \;\; w_2(\xi) := v \times w_1(\xi), \;\; w_3(\xi) := v.$$

Notice that $w_1(\xi)$ and $w_2(\xi)$ span the 2-space perpendicular to v.

Definition 5 (Special orthonormal frames). For any given $\xi = (q, v) \in N$ we refer to

$$(e_1(q), e_2(q), e_3(q)), \;\; (u_1(q), u_2(q), u_3(q)), \;\; (w_1(\xi), w_2(\xi), w_3(\xi))$$

as the *product frame*, the *eigenframe*, and the *wavefront frame*, respectively.

3. Period-2 orbits

Much of the following discussion will be around period-2 orbits. The existence of periodic orbits for no-slip billiards is in general harder to establish than for the standard billiard

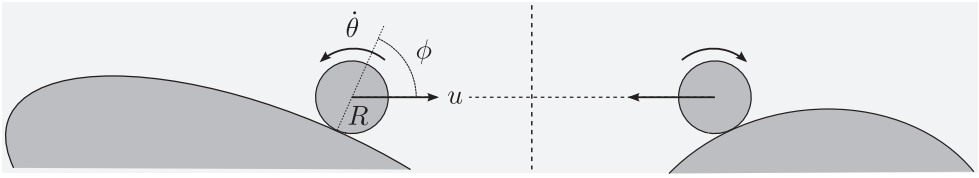

Figure 5. For a period-2 orbit, the velocity u of the center of mass and the angular velocity $\dot{\theta}$ are related by $|\dot{\theta}| = (mR/\mathscr{I})|u \sin\phi|$, where m is the disc's mass, $\mathscr{I}$ is its moment of inertia, and its radius is R.

systems, despite numerical evidence that these orbits are very common; on the other hand, period-2 orbits are often easily obtained, as we indicate in this section.

Let $\xi = (q, v)$ be the initial state of a periodic orbit of period 2, $\tilde{\xi} = (\tilde{q}, \tilde{v}) = T(\xi)$, and t the time of free flight between collisions. Then,

$$(q, v) = (\tilde{q} + tC_{\tilde{q}}v, C_q\tilde{v}) = (q + t(v + C_{\tilde{q}}v), C_qC_{\tilde{q}}v)$$

so that $C_{\tilde{q}}v = -v$ and $v = C_qC_{\tilde{q}}v$. Because v and $u_1(q)$ (respectively, $u_1(\tilde{q})$) are eigenvectors for different eigenvalues of the orthogonal map C_q (respectively, $C_{\tilde{q}}$), v is perpendicular to both $u_1(q)$ and $u_1(\tilde{q})$. It follows from (2) that $u_1(q) \cdot e_1 = u_1(\tilde{q}) \cdot e_1$. Thus the projection of e_1 to $v^\perp$ is proportional to $u_1(q) + u_1(\tilde{q})$. By the definition of the wavefront vector $w_1(\xi)$ (and the angle ϕ, see figure 4) we have

$$w_1(\xi) = w_1(\tilde{\xi}) = \frac{u_1(q) + u_1(\tilde{q})}{|u_1(q) + u_1(\tilde{q})|} = \frac{u_1(q) + u_1(\tilde{q})}{2\sqrt{1 - \cos^2(\beta/2)\cos^2\phi}}.$$

Now observe that $u_1(\tilde{q}) - u_1(q)$ is perpendicular to $u_1(q) + u_1(\tilde{q})$. It follows from this remark and a glance at figure 4 (to determine the orientation of the vectors) that

$$w_2(\xi) = -w_2(\tilde{\xi}) = \frac{u_1(\tilde{q}) - u_1(q)}{|u_1(\tilde{q}) - u_1(q)|} = \frac{u_1(\tilde{q}) - u_1(q)}{2\cos(\beta/2)\cos\phi}.$$

Notice, in particular, that v is a positive multiple of $u_1(q) \times u_1(\tilde{q})$. (See figure 6.) An elementary calculation starting from this last observation gives v in terms of the product frame:

$$v = \frac{\cos(\beta/2)\sin\phi\, e_1 + \sin(\beta/2)\,[\sin\phi e_2(q) + \cos\phi\, e_3(q)]}{\sqrt{1 - \cos^2(\beta/2)\cos^2\phi}}.$$

A more physical description of the velocity v of a period-2 orbit is shown in figure 5.

Equally elementary computations yield the collision map C_q in the wavefront frame at q, for a period-2 state $\xi = (q, v)$. We register this here for later use. To shorten the equations we write $c_{\beta/2} = \cos(\beta/2)$ and $c_\phi = \cos\phi$.

$$\begin{aligned}
C_q w_1(\xi) &= \left(1 - 2c_{\beta/2}^2 c_\phi^2\right) w_1(\xi) - 2c_{\beta/2}c_\phi\sqrt{1 - c_{\beta/2}^2 c_\phi^2}\, w_2(\xi)\\
C_q w_2(\xi) &= -2c_{\beta/2}c_\phi\sqrt{1 - c_{\beta/2}^2 c_\phi^2}\, w_1(\xi) - \left(1 - 2c_{\beta/2}^2 c_\phi^2\right) w_2(\xi)\\
C_q w_3(\xi) &= -w_3(\xi).
\end{aligned} \tag{3}$$

The following easily obtained inner products will also be needed later.

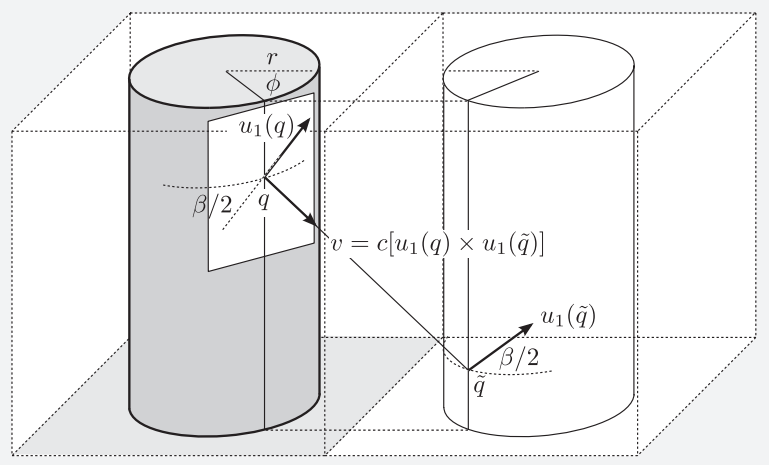

Figure 6. Notation used in this section is illustrated here with the configuration manifold of the no-slip Sinai billiard. (See section 9 and 3.) The shaded half of the figure is meant to indicate a fundamental domain in $\mathbb{R}^3$ that projects to M in the 3-torus and on the right-hand side, without shading, is a translate. The pair (q, v) as shown in this figure is the initial state of a period-2 orbit parametrized by the angle φ.

$$\begin{aligned} u_1(\tilde{q}) \cdot u_1(q) &= 1 - 2\cos^2(\beta/2)\cos^2\phi \\ w_1(\xi) \cdot u_1(q) &= \sqrt{1 - \cos^2(\beta/2)\cos^2\phi} \\ w_2(\xi) \cdot u_1(q) &= -\cos(\beta/2)\cos\phi. \end{aligned} \tag{4}$$

The notation used above is illustrated in figure 6. The configuration manifold M of the no-slip Sinai billiard is the complement in $\mathbb{T}^3$ of the Cartesian product of the scatterer disc and $\mathbb{T}^1$. The figure shows two fundamental domains in $\mathbb{R}^3$ that project to M and an orbit segment connecting the points q and $\tilde{q}$ having velocity v at q. As explained above, when v has the form shown in figure 6, it generates a period-2 orbit. The projection of this orbit to $\mathscr{B}$ is shown on the left-hand side of figure 13. Notice that the vector v is parametrized by the angle $\phi \in (-\pi/2, \pi/2)$. Therefore we have in this case a one-parameter family of initial conditions giving period-2 orbits, parametrized by ϕ. Linear stability of the orbits in this one-parameter family will be studied in section 9.

4. The differential of the no-slip billiard map

Mostly, in this section, we write $\langle u, v\rangle$ instead of $u \cdot v$ for the standard inner product of $\mathbb{R}^3$. Let $q(s)$ be a smooth curve in ∂M such that $q(0) = q$ and $q'(0) = X \in T_q(\partial M)$. Define

$$\omega_q(X) := \frac{\mathrm{d}}{\mathrm{d}s}\bigg|_{s=0} \sigma(q(0))^{-1}\sigma(q(s)) \in \mathfrak{so}(3)$$

where $\mathfrak{so}(3)$ is the space of antisymmetric 3×3 matrices (the Lie algebra of the rotation group) and $\sigma(q) := \sigma_q$ is the product frame. As the field e_1 is constant and $\omega_q(X)$ is antisymmetric we have $\omega_q(X)_{ij} = 0$ except possibly for $(i, j) = (2, 3)$ and $(3, 2)$. Denoting by D_X directional derivative of vector fields along X at q,

$$\omega_q(X)_{23} = \epsilon_2 \cdot \left[\frac{\mathrm{d}}{\mathrm{d}s}\bigg|_{s=0} \sigma(q(0))^{-1}\sigma(q(s))\epsilon_3 \right] = \langle e_2(q), D_X e_3\rangle = \langle e_2(q), X\rangle \left\langle e_2(q), D_{e_2(q)} e_3 \right\rangle$$

since $D_{e_1} e_3 = 0$. The inner product $\kappa(q) := \left\langle e_2(q), D_{e_2(q)} e_3 \right\rangle$ is the geodesic curvature of the boundary of $\mathscr{B}$ at $\bar{q}$, where $\bar{q}$ is the base point of q in $\partial\mathscr{B}$. Thus

$$\omega_q(X) = \kappa(q)\langle e_2(q), X\rangle \mathscr{A} \tag{5}$$

where

$$\mathscr{A} = \begin{pmatrix} 0 & 0 & 0 \\ 0 & 0 & 1 \\ 0 & -1 & 0 \end{pmatrix}.$$

Given vector fields μ, ν, it is convenient to define $\mu \odot \nu$ as the map

$$(q, v) \mapsto (\mu \odot \nu)_q v := \langle \mu_q, v\rangle \nu_q + \langle \nu_q, v\rangle \mu_q. \tag{6}$$

Lemma 6. *The directional derivative of C along $X \in T_q(\partial M)$ is*

$$D_X C = \kappa(q)\, \langle e_2(q), X\rangle\, \mathscr{O}_q$$

where $\mathscr{O}_q := \sigma_q \mathscr{O} \sigma_q^{-1}$, $\mathscr{O}$ is the commutator of $\mathscr{A}$ and $\mathscr{C}$ given by

$$\mathscr{O} := \mathscr{A}\mathscr{C} - \mathscr{C}\mathscr{A} = 2\cos(\beta/2) \begin{pmatrix} 0 & 0 & \sin(\beta/2) \\ 0 & 0 & -\cos(\beta/2) \\ \sin(\beta/2) & -\cos(\beta/2) & 0 \end{pmatrix}$$

and $\mathscr{C}$ was defined above in (1). Furthermore, $\mathscr{O}_q = 2\cos(\beta/2)(u_1 \odot e_3)_q$ and

$$D_X C = 2\cos(\beta/2)\kappa(q)\langle X, e_2\rangle_q (u_1 \odot e_3)_q.$$

Proof. Notice that $0 = D_X I = D_X(\sigma^{-1}\sigma) = (D_X\sigma^{-1})\sigma + \sigma^{-1} D_X \sigma$. Thus

$$D_X \sigma^{-1} = -\sigma^{-1}\, (D_X \sigma)\, \sigma^{-1}.$$

Therefore,

$$D_X C = (D_X\sigma)\mathscr{C}\sigma^{-1} + \sigma\mathscr{C} D_X\sigma^{-1} = \sigma\left[\sigma^{-1} D_X \sigma\right]\mathscr{C}\sigma^{-1} - \sigma\mathscr{C}\left[\sigma^{-1} D_X\sigma\right]\sigma^{-1} = \sigma[\omega(X), \mathscr{C}]\sigma^{-1}.$$

The first claimed expression for $D_X C$ is now a consequence of equation (5). A simple computation also gives, for any given $v \in \mathbb{R}^3$,

$$\mathscr{O}_q v = 2\cos(\beta/2)(e_3 \odot u_1)_q v \tag{7}$$

yielding the second expression for $D_X C$. □

It is also convenient to define the following two projections. Let $\xi = (q, v) \in N^{\pm}$. The space $T_\xi N^{\pm}$ decomposes as a direct sum $T_\xi N^{\pm} = H_\xi \oplus V_\xi$ where

$$H_\xi = T_q(\partial M) = \{X \in \mathbb{R}^3 : X \cdot e_3(q) = 0\} \text{ and } V_\xi = v^{\perp} = \{Y \in \mathbb{R}^3 : Y \cdot v = 0\}.$$

We refer to these as the *horizontal* and *vertical* subspaces of $T_\xi N^{\pm}$. We use the same symbols to denote the projections $H_\xi : \mathbb{R}^3 \to T_q(\partial M)$ and $V_\xi : \mathbb{R}^3 \to v^{\perp}$ defined by

$$H_\xi Z := Z - \frac{\langle Z, e_3(q)\rangle}{\langle v, e_3(q)\rangle} v, \quad V_\xi Z := Z - \langle Z, v\rangle v.$$

We note that for $\xi = (q, v) \in N^\pm$ and $Z \in \mathbb{R}^3$

$$\langle e_2(q), H_\xi Z\rangle = \frac{\langle Z, e_2(q)\rangle\langle v, e_3(q)\rangle - \langle Z, e_3(q)\rangle\langle v, e_2(q)\rangle}{\langle v, e_3(q)\rangle} = \frac{\langle v \times e_1(q), Z\rangle}{\langle v, e_3(q)\rangle}.$$

Also observe that $v \times e_1 = |\overline{v}| w_2(\xi)$, where w_2 is the second vector in the wavefront frame (see definition 5) and $\overline{v}$ is the orthogonal projection of v to the plane perpendicular to e_1. Thus, denoting by $\phi(\xi)$ the angle between $\overline{v}$ and $e_3(q)$ (this is the same ϕ as in figures 4–6)

$$\langle e_2(q), H_\xi Z\rangle = \frac{1}{\cos\phi(\xi)}\langle w_2(\xi), Z\rangle. \tag{8}$$

Let $q \in \partial M$, $v = v_- \in N_q^-$, $v_+ := C_q v_- \in N_q^+$, $\xi = \xi_- = (q, v_-)$, $\xi_+ = (q, v_+)$. Define

$$\Lambda_\xi := V_{\xi_+} H_{\xi_-} : v_-^\perp \to v_+^\perp. \tag{9}$$

Clearly Λ_ξ is defined on all of $\mathbb{R}^3$, not only on $v_-^\perp$, but we are particularly interested in its restriction to the latter subspace.

Let $\xi = (q, v)$ be a point contained in a neighborhood of N where T is defined and differentiable. Set $\tilde{\xi} = T(\xi)$. We wish to describe $\mathrm{d}T_\xi : T_\xi N \to T_{\tilde{\xi}} N$. Let $\xi(s) = (q(s), v(s))$ be a differentiable curve in N with $\xi(0) = \xi$ and define

$$X := q'(0) \in T_q N, \quad Y := v'(0) \in v^\perp.$$

Then $\tilde{\xi}(s) = T(\xi(s)) = (\tilde{q}(s), \tilde{v}(s)) \in N$ where $\tilde{q}(s) = q(s) + t(s)v(s)$ and $\tilde{v}(s) = C_{\tilde{q}(s)} v(s)$. From the equality $\langle \tilde{q}'(0), e_3(\tilde{q})\rangle = 0$ it follows that

$$t'(0) = -\frac{\langle X + tY, e_3(\tilde{q})\rangle}{\langle v, e_3(\tilde{q})\rangle}.$$

Consequently, $\tilde{X} := \tilde{q}'(0) \in T_{\tilde{q}} N$ and $\tilde{Y} := \tilde{v}'(0) \in \tilde{v}^\perp$ satisfy

$$\tilde{X} = X + tY - \frac{\langle X + tY, e_3(\tilde{q})\rangle}{\langle v, e_3(\tilde{q})\rangle} v = H_{\tilde{\xi}_-}(X + tY)$$

and

$$\tilde{Y} = C_{\tilde{q}} Y + \left[\frac{\mathrm{d}}{\mathrm{d}s}\bigg|_{s=0} C_{\tilde{q}(s)}\right] v = C_{\tilde{q}} Y + \kappa(\tilde{q})\langle e_2(\tilde{q}), \tilde{X}\rangle \mathscr{O}_{\tilde{q}} v$$

where we have used lemma 6. From the same lemma, $\mathscr{O}_q v = -2\cos(\beta/2)(\nu \odot u_1)_{\tilde{q}} v$. Thus

$$\begin{aligned} \tilde{X} &= H_{\tilde{\xi}_-}(X + tY) \\ \tilde{Y} &= C_{\tilde{q}} Y - 2\cos(\beta/2)\kappa(\tilde{q})\left\langle e_2(\tilde{q}), H_{\tilde{\xi}_-}(X + tY)\right\rangle (\nu \odot u_1)_{\tilde{q}} v. \end{aligned} \tag{10}$$

As already noted, $T_\xi N^+ = T_q(\partial M) \oplus v^\perp$. By using the projection $V_\xi : T_q(\partial M) \to v^\perp$ introduced earlier we may identify $T_\xi N^+$ with the sum $v^\perp \oplus v^\perp$. In this way $\mathrm{d}T_\xi$ is regarded as a map from $v^\perp \oplus v^\perp$ to $\tilde{v}^\perp \oplus \tilde{v}^\perp$.

Proposition 7. *Let $T : N \to N$ be the billiard map, $\xi = (q, v) \in N$ and $(\tilde{q}, \tilde{v}) = \tilde{\xi} = T(\xi)$, where $\tilde{q} = q + tv$, and $\tilde{v} = C_{\tilde{q}} v$. Under the identification of the tangent space $T_\xi N$ with $v^\perp \oplus v^\perp$*

as indicated just above, we may regard the differential $\mathrm{d}T_\xi$ *as a linear map from* $v^\perp \oplus v^\perp$ *to* $\tilde{v}^\perp \oplus \tilde{v}^\perp$. *Also recall from (8) the definition of* $\Lambda_{\tilde{\xi}} : v^\perp \to \tilde{v}^\perp$. *Then* $\mathrm{d}T_\xi : T_\xi N \to T_{\tilde{\xi}} N$ *is given by*

$$\begin{pmatrix} X \\ Y \end{pmatrix} \mapsto \begin{pmatrix} \Lambda_{\tilde{\xi}}(X + tY) \\ C_{\tilde{q}} Y + 2\cos(\beta/2)\kappa(\tilde{q}) \frac{(e_3 \odot u_1)_{\tilde{q}} v}{\cos\phi(\tilde{q}, v)} \langle w_2(\xi), X + tY \rangle \end{pmatrix}$$

where $\cos\phi(\tilde{q}, v) = \langle \overline{v}/|\overline{v}|, e_3(\tilde{q}) \rangle$ *and* $\overline{v}$ *is the orthogonal projection of* v *to* $e_1^\perp$.

Proof. This is a consequence of the preceding remarks and definitions. □

Corollary 8. *If* $\xi = (q, v)$ *is periodic of period 2, then* $C_{\tilde{q}} v = -v$, $\langle v, u_1(\tilde{q}) \rangle = 0$, *and the map of proposition 7 reduces to*

$$\begin{pmatrix} X \\ Y \end{pmatrix} \mapsto \begin{pmatrix} X + tY \\ C_{\tilde{q}} Y + 2\cos(\beta/2)\kappa(\tilde{q}) \frac{\cos\psi(\tilde{q}, v)}{\cos\phi(\tilde{q}, v)} \langle w_2(\xi), X + tY \rangle u_1(\tilde{q}) \end{pmatrix}$$

where $\cos\psi(\tilde{q}, v) := \langle v, e_3(\tilde{q}) \rangle$, $\cos\phi(\tilde{q}, v) = \langle \overline{v}/|\overline{v}|, e_3(\tilde{q}) \rangle$.

Proof. Clearly, $C_{\tilde{q}} v = -v$, whence $\langle v, u_1(\tilde{q}) \rangle = 0$ and $(e_3 \odot u_1)_{\tilde{q}} v = \langle e_3(\tilde{q}), v \rangle u_1(\tilde{q})$. Also notice that $\Lambda_{\tilde{\xi}} Z = Z$ whenever $\langle Z, v \rangle = 0$. The corollary follows. □

5. Measure invariance and time reversibility

It will be seen below that the no-slip billiard map does not preserve the natural symplectic form on N, so these systems are not Hamiltonian. Nevertheless, the canonical billiard measure derived from the symplectic form (the Liouville measure) is invariant and the system is time reversible, so some of the good features of Hamiltonian systems are still present. (It is interesting to note in this regard that in [10, 11] a KAM theory is developed for reversible systems.)

Recall that an invertible map T is said to be *reversible* if there exists an involution $\mathscr{R}$ such that

$$\mathscr{R} \circ T \circ \mathscr{R} = T^{-1}.$$

In order to see that the no-slip billiard map T is reversible we first define the following maps: $\Phi : (q, v) \mapsto (q + tv, v)$, where t is the time of free motion of the trajectory with initial state (q, v), so that $q, q + tv \in \partial M$; the collision map $C : N \to N$ given by $C(q, v) = (q, C_q v)$; and the flip map $J : (q, v) \mapsto (q, -v)$ where $q \in \partial M$ and $v \in \mathbb{R}^3$. Recall that $T = C \circ \Phi$. Now set $\mathscr{R} := J \circ C = C \circ J$. It is clear (since C_q is an involution by proposition 3) that $\mathscr{R}^2 = I$ and that $J \circ \Phi \circ J = \Phi^{-1}$. Therefore,

$$\mathscr{R} \circ T \circ \mathscr{R} = J \circ C^2 \circ \Phi \circ J \circ C = J \circ \Phi \circ J \circ C = \Phi^{-1} \circ C = (C \circ \Phi)^{-1} = T^{-1}.$$

Notice that if $L : V \to V$ is a reversible isomorphism of a vector space V with time reversal map $\mathscr{R} : V \to V$ (so that $\mathscr{R} \circ L \circ \mathscr{R} = L^{-1}$) then for any eigenvalue λ of L associated to eigenvector u, $1/\lambda$ is also an eigenvalue for the eigenvector $\mathscr{R}u$, as easily checked. These elementary observations have the following useful consequence.

Proposition 9. *Let $\xi \in N$ be a periodic point of period k of the no-slip billiard system and let λ be an eigenvalue of the differential map $\mathrm{d}T_\xi^k : T_\xi N \to T_\xi N$ corresponding to eigenvector u. Then $1/\lambda$ is also an eigenvalue of $\mathrm{d}T_\xi^k$ corresponding to eigenvector $\mathscr{R}u$, where $\mathscr{R}$ is the composition of the collision map C and the flip map J. Furthermore, e_1 (see definition 5) is always an eigenvector of $\mathrm{d}T_\xi$ and all its powers, corresponding to the eigenvalue* 1.

We now turn to invariance of the canonical measure. The canonical 1-form θ on N is defined by

$$\theta_\xi(U) := v \cdot X$$

for $\xi = (q, v) \in N$ and $U = (X, Y) \in T_qN \oplus v^\perp = T_\xi N$. Its differential $\mathrm{d}\theta$ is a symplectic form on $N \cap \{v \in T_q(\partial M) : |v| = 1\}^c$ and $\Omega = \mathrm{d}\theta \wedge \mathrm{d}\theta$ is the canonical volume form on this same set. In terms of horizontal and vertical components of vectors in TN, the symplectic form is expressed as

$$\mathrm{d}\theta(U_1, U_2) = Y_1 \cdot X_2 - Y_2 \cdot X_1$$

where $U_i = (X_i, Y_i)$. An elementary computation shows that the measure on N associated to Ω is given by

$$|\Omega_\xi| = v \cdot \nu(q)\, \mathrm{d}A_{\partial M}(q)\, \mathrm{d}A_N(v) \tag{11}$$

where $\nu(q) := e_3(q)$, $\mathrm{d}A_{\partial M}(q)$ is the area measure on ∂M, and $\mathrm{d}A_N(v)$ is the area measure on the hemisphere $N_q = \{v \in \mathbb{R}^3 : v \cdot \nu(q) > 0\}$.

Proposition 10. *The canonical 4-form Ω on N transforms under the no-slip billiard map as $T^*\Omega = -\Omega$. In particular, the associated measure $|\Omega|$, shown explicitly in equation 11, is invariant under T.*

Proof. Let u be a vector field on ∂M and introduce the one-form θ^u on N given by

$$\theta^u_\xi(U) := (v \cdot u(q))(u(q) \cdot X)$$

for $\xi = (q, v)$ and $U = (X, Y)$. Taking u to be each of the vector fields u_1, u_2 we obtain the 1-forms θ^{u_1} and θ^{u_2}. As $v = (v \cdot u_1)u_1 + (v \cdot u_2)u_2 + (v \cdot \nu)\nu$ and $X \cdot \nu = 0$, we have

$$\theta = \theta^{u_1} + \theta^{u_2}.$$

The no-slip collision map C acts on $u = \theta^{u_i}$ as follows: For $U = (X, Y) \in T_q(\partial M) \oplus v^\perp$,

$$(C^*\theta^u)_\xi(U) = (C_q(v) \cdot u(q))(u(q) \cdot X) = (v \cdot C_q(u(q)))(u(q) \cdot X)$$

where C^* denotes the pull-back operation on forms. It follows that

$$C^*\theta^{u_1} = \theta^{u_1}, \quad C^*\theta^{u_2} = -\theta^{u_2}.$$

We now compute the differentials $\mathrm{d}\theta^u$ for $u = u_1, u_2$. Observe that $\theta^u = f^u(\xi)(\pi^* u^\flat)$, where f^ξ is the function on N defined by $f^u(\xi) := v \cdot u(q)$ and $\pi^* u^\flat$ is the pull-back under the projection map $\pi : N \to \partial M$ of the 1-form $u^\flat$ on ∂M given by $u^\beta_q(X) = u(q) \cdot X$. Thus

$$\mathrm{d}\theta^u = \mathrm{d}f^u \wedge (\pi^* u^\flat) + f^u \pi^* \mathrm{d}u^\flat.$$

A simple calculation gives

$$\mathrm{d}f^u_\xi(X, Y) = v \cdot (D_X u) + u(q) \cdot Y.$$

The vector field $u = u_i$ is parallel on ∂M. In fact, its derivative in direction $X \in T_q(\partial M)$ only has component in the normal direction, given by

$$D_X u = \kappa(q)(X \cdot e_2(q))(u(q) \cdot e_2(q))\nu(q).$$

Omitting the dependence on q, we have

$$\mathrm{d}f^u_\xi(X, Y) = \kappa(q)(X \cdot e_2)(u \cdot e_2)(v \cdot \nu) + u \cdot Y.$$

Another simple calculation gives

$$\mathrm{d}u^\flat_q(X_1, X_2) = (D_{X_1} u) \cdot X_2 - (D_{X_2} u) \cdot X_1 = 0$$

so $\mathrm{d}\theta^u = \mathrm{d}f^u \wedge \pi^* u^\flat$. Explicitly,

$$\mathrm{d}\theta^u(U_1, U_2) = (u \cdot Y_1)(u \cdot X_2) - (u \cdot Y_2)(u \cdot X_1) - \kappa(q)(v \cdot \nu)(u \cdot e_1)(u \cdot e_2)\omega(X_1, X_2)$$

where

$$\omega(X_1, X_2) := (e_1 \cdot X_1)(e_2 \cdot X_2) - (e_2 \cdot X_1)(e_1 \cdot X_2).$$

Notice that ω is the area form on ∂M. A convenient way to express $\mathrm{d}\theta^u$ is as follows. Define the 1-form $\tilde{u}$ on N by $\tilde{u}_\xi(U) = u(q) \cdot Y$, where $U = (X, Y) \in T_\xi N$, and the function $g^u(\xi) := -\kappa(q)(v \cdot \nu)(u \cdot e_1)(u \cdot e_2)$. These extra bits of notation now allow us to write

$$\mathrm{d}\theta^u_\xi = g^u(\xi)(\pi^*\omega) + \tilde{u} \wedge (\pi^* u^\flat).$$

The main conclusion we wish to derive from these observations is that $\mathrm{d}\theta^u \wedge \mathrm{d}\theta^u = 0$. This is the case because, as $\dim(\partial M) = 2$, we must have $\omega^2 = 0$ and $\omega \wedge u^\flat = 0$. Therefore,

$$\Omega := \mathrm{d}\theta \wedge \mathrm{d}\theta = (\mathrm{d}\theta^{u_1} + \mathrm{d}\theta^{u_2}) \wedge (\mathrm{d}\theta^{u_1} + \mathrm{d}\theta^{u_2}) = 2\mathrm{d}\theta^{u_1} \wedge \mathrm{d}\theta^{u_2}.$$

Finally,

$$C^*\Omega = 2d(C^*\theta^{u_1}) \wedge d(C^*\theta^{u_2}) = -2\mathrm{d}\theta^{u_1} \wedge \mathrm{d}\theta^{u_2} = -\Omega.$$

The forms $\mathrm{d}\theta$ and Ω are invariant under the geodesic flow and under the map it induces on N. As T is the composition of this map and C, the proposition is established. □

6. Wedge billiards

One of the main observations of this paper is that a wedge billiard (as in figure 7) always contains, arbitrarily near its corner, period-2 orbits which are Lyapunov stable. This then implies the existence of such stable orbits for most polygonal billiards. This is proved in the present section.

We set the following conventions for a wedge table with corner angle 2ϕ. See figure 7. (This is the same ϕ that has appeared before in previous figures.) The boundary planes of the configuration manifold are denoted $\mathscr{P}_1$ and $\mathscr{P}_2$. The orthonormal vectors of the constant product frame on plane $\mathscr{P}_i$ are $e_{1,i}, e_{2,i}, e_{3,i} = \nu_i$ for $i = 1, 2$ where

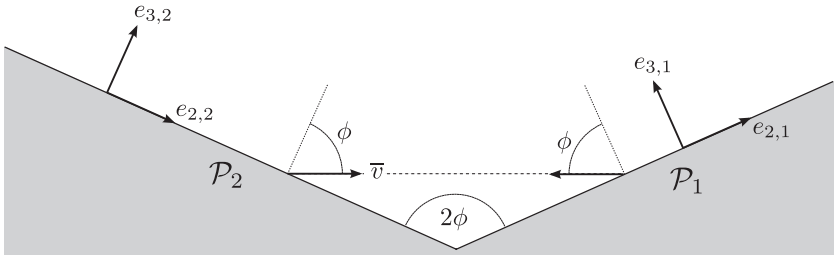

Figure 7. Some notation specific to the wedge billiard table. The $\mathscr{P}_i$ are the half-plane components of the boundary of the configuration manifold.

$$e_{1,1} = \begin{pmatrix} 0 \\ 0 \\ 1 \end{pmatrix}, \quad e_{2,1} = \begin{pmatrix} \cos\phi \\ -\sin\phi \\ 0 \end{pmatrix}, \qquad e_{3,1} = \begin{pmatrix} \sin\phi \\ \cos\phi \\ 0 \end{pmatrix},$$

$$e_{1,2} = \begin{pmatrix} 0 \\ 0 \\ 1 \end{pmatrix}, \quad e_{2,2} = -\begin{pmatrix} \cos\phi \\ \sin\phi \\ 0 \end{pmatrix}, \quad e_{3,2} = \begin{pmatrix} \sin\phi \\ -\cos\phi \\ 0 \end{pmatrix}.$$

Let $\sigma_i : \mathbb{R}^3 \to T_q \oplus \mathbb{R}\nu_i$ be the constant orthogonal map such that $\sigma_i \epsilon_j = e_{j,i}$, where ϵ_i, $i = 1, 2, 3$, is our notation for the standard basis vectors in $\mathbb{R}^3$. Let

$$u_{1,i} = \sin(\beta/2)e_{1,i} - \cos(\beta/2)e_{2,i}, \;\; u_{2,i} = \cos(\beta/2)e_{1,i} + \sin(\beta/2)e_{2,i}, \;\; u_{3,i} = e_{3,i} = \nu_i$$

be the eigenvectors of the no-slip reflection map associated to the plane $\mathscr{P}_i$ and set $\zeta_i \epsilon_j := u_{j,i}$. For easy reference we record their matrices here:

$$\zeta_i = \begin{pmatrix} (-1)^i \cos(\beta/2)\cos\phi & -(-1)^i \sin(\beta/2)\cos\phi & \sin\phi \\ \cos(\beta/2)\sin\phi & -\sin(\beta/2)\sin\phi & -(-1)^i\cos\phi \\ \sin(\beta/2) & \cos(\beta/2) & 0 \end{pmatrix}.$$

The initial velocity v for the period-2 trajectory points in the direction of $u_{1,2} \times u_{1,1}$ and is given by

$$v = \frac{1}{\sqrt{1 - \cos^2(\beta/2)\cos^2\phi}} \begin{pmatrix} 0 \\ \sin(\beta/2) \\ \cos(\beta/2)\sin\phi \end{pmatrix}.$$

This periodic trajectory connects the points $q_1 \in \mathscr{P}_1$ and $q_2 \in \mathscr{P}_2$. Any such pair of points can be written as

$$q_1 = a \begin{pmatrix} \sin(\beta/2)\cos\phi \\ -\sin(\beta/2)\sin\phi \\ b - \cos(\beta/2)\sin^2\phi \end{pmatrix}, \;\; q_2 = a \begin{pmatrix} \sin(\beta/2)\cos\phi \\ \sin(\beta/2)\sin\phi \\ b + \cos(\beta/2)\sin^2\phi \end{pmatrix}$$

where $a, b \in \mathbb{R}$, $a > 0$. In what follows we assume without loss of generality that $a = 1$ and $b = 0$. Thus

$$q_i = \left(\sin(\beta/2)\cos\phi, (-1)^i \sin(\beta/2)\sin\phi, (-1)^i \cos(\beta/2)\sin^2\phi\right)^t.$$

Let $S_i^{\pm} = \{v \in \mathbb{R}^3 : |v| = 1, \pm v \cdot \nu_i > 0\}$. The collision maps $C_i : S_i^- \to S_i^+$, $i = 1, 2$ are given by the matrices

$$C_i = \sigma_i \mathscr{C} \sigma_i^{-1} = \zeta_i \begin{pmatrix} 1 & 0 & 0 \\ 0 & -1 & 0 \\ 0 & 0 & -1 \end{pmatrix} \zeta_i^{-1}$$

where $\mathscr{C}$ was defined in equation (1). We now introduce coordinates on $\mathscr{P}_i \times S_i^+$ as follows. Let $S_+^2 = \{z \in \mathbb{R}^3 : |z| = 1, z_3 > 0\}$ and define $\Phi_i : \mathbb{R}^2 \times S_+^2 \to \mathscr{P}_i \times S_i^+$ by

$$\Phi_i(x, z) = (q_i + \zeta_i x, \zeta_i z)$$

where we regard $x \in \mathbb{R}^2$ as $(x, 0) \in \mathbb{R}^3$. This same map may also be written as follows (here we use the indices in x_i and z_i to indicate coordinates of $x = (x_1, x_2)$ and $z = (z_1, z_2, z_3)$; elsewhere in this section such indices indicate different vectors):

$$\Phi_i(x, z) = (q_i + x_1 u_{1,i} + x_2 u_{2,i}, z_1 u_{1,i} + z_2 u_{2,i} + z_3 u_{3,i}) .$$

Clearly, the billiard map is not defined on all of $\bigcup_i \mathscr{P}_i \times S_i^+$ since those initial velocities not pointing towards the other plane will escape to infinity, but we are interested in the behavior of the map on a neighborhood of the periodic point $\xi_i = (q_i, v_i)$, $v_i = -(-1)^i v$. The question of interest here is whether some open neighborhood of ξ_i remains invariant under the billiard map. It is easily shown that the coordinates of the state ξ_i (of the period-2 orbit at the plane $\mathscr{P}_i$) are $\Phi_i^{-1}(\xi_i) = (0, y_i) \in \mathbb{R}^2 \times S_+^2$ where

$$y_i = \frac{1}{\sqrt{1 - \cos^2(\beta/2)\cos^2\phi}} \left(0, (-1)^i \sin\phi, \sin(\beta/2)\cos\phi\right)^t .$$

Let $T_i : \mathscr{D}_i \subset \mathbb{R}^2 \times S_+^2 \to \mathbb{R}^2 \times S_+^2$ be the billiard map restricted to $\mathscr{P}_i \times S_i^+$ expressed in the coordinate system defined by Φ_i. Thus

$$T_1 = \Phi_2^{-1} T \Phi_1, \quad T_2 = \Phi_1^{-1} T \Phi_2$$

on their domains $\mathscr{D}_i$. We now find the explicit form of T_i. Define $\bar{i} = \begin{cases} 1 & \text{if } i = 2 \\ 2 & \text{if } i = 1 \end{cases}$ and orthogonal matrices $A_i := \zeta_{\bar{i}}^{-1} \zeta_i$ and $S = \operatorname{diag}(1, -1, -1)$, both in $SO(3)$. Also define

$$\alpha := 2 \sin\phi \sqrt{1 - \cos^2(\beta/2)\cos^2\phi}.$$

Observe that $\zeta_{\bar{i}}^{-1} C_{\bar{i}} \zeta_i = SA_i$. It is easily shown that

$$q_i - q_{\bar{i}} = -\alpha v_i, \; v_i = \zeta_i y_i, \; A_i y_i = -y_{\bar{i}}, \; SA_i y_i = y_{\bar{i}}.$$

In particular, $\zeta_{\bar{i}}^{-1}(q_i - q_{\bar{i}}) = -\alpha y_i$. Let $Q : \mathbb{R}^3 \times S_+^2 \to \mathbb{R}^2$ be defined by

$$Q(x, y) := x - \frac{x \cdot \epsilon_3}{y \cdot \epsilon_3} y.$$

Notice that $Q(x, y) \cdot \epsilon_3 = 0$. We now have

$$T_i : (x, y) \mapsto \left(Q\left(A_i(x - \gamma y_i), A_i y\right), SA_i y\right) . \tag{12}$$

For easy reference we record

$$\alpha y_i = 2\sin\phi \begin{pmatrix} 0 \\ (-1)^i \sin\phi \\ \sin(\beta/2)\cos\phi \end{pmatrix}, \quad S = \begin{pmatrix} 1 & 0 & 0 \\ 0 & -1 & 0 \\ 0 & 0 & -1 \end{pmatrix}$$

and

$$A_2 = A_1^t = \zeta_1^{-1}\zeta_2 = \begin{pmatrix} 1 - 2\cos^2(\beta/2)\cos^2\phi & -\sin\beta\cos^2\phi & \cos(\beta/2)\sin(2\phi) \\ -\sin\beta\cos^2\phi & 1 - 2\sin^2(\beta/2)\cos^2\phi & \sin(\beta/2)\sin(2\phi) \\ -\cos(\beta/2)\sin(2\phi) & -\sin(\beta/2)\sin(2\phi) & -\cos(2\phi) \end{pmatrix}.$$

Using the notation $[z]_3 := z \cdot \epsilon_3$ and elementary computations based on the above gives:

Proposition 11. *The return map in the coordinate system defined by* Φ_1 *has the form*

$$T_2T_1(x,y) = (x + [A_1(x - \alpha y_1)]_3 V(y), SA_1^t SA_1 y)$$

where

$$V(y) = \frac{[y]_3 A_1^t SA_1 y - [A_1^t SA_1 y]_3 y}{[A_1 y]_3 [A_1^t SA_1 y]_3}.$$

This vector satisfies: $[V(y)]_3 = 0$ *and* $V(y_1) = 0$. *In particular,* $T_2T_1(x, y_1) = (x, y_1)$ *whenever (x, y1) is in the domain of* T_2T_1.

In order to study this return map in a neighborhood of (x,y_1) we use spherical coordinates about the axis y_1:

$$y = \cos\psi\, y_1 + \sin\psi\cos\varphi\,\hat{\epsilon}_1 + \sin\psi\sin\varphi\,\hat{\epsilon}_2 \tag{13}$$

where

$$\hat{\epsilon}_1 := \epsilon_1, \quad \hat{\epsilon}_2 := \frac{1}{\sqrt{1 - \cos^2(\beta/2)\cos^2\phi}}(\sin(\beta/2)\cos\phi\,\epsilon_2 + \sin\phi\,\epsilon_3), \quad \hat{\epsilon}_3 := y_1$$

form an orthonormal frame. See figure 8. (Notice the typographical distinction between the corner angle ϕ of the wedge domain and the spherical coordinate φ.) Let

$$(X(x,\varphi,\psi), Y(x,\varphi,\psi)) := T_2T_1(x, \cos\psi\, y_1 + \sin\psi\cos\varphi\,\hat{\epsilon}_1 + \sin\psi\sin\varphi\,\hat{\epsilon}_2)$$

and define

$$w := w(\varphi) := \cos\varphi\,\hat{\epsilon}_1 + \sin\varphi\,\hat{\epsilon}_2.$$

Thus we may write $y = \cos\psi\,(y_1 + \tan\psi w(\varphi))$. Since the rotation $S_2 := SA_1^t SA_1$ fixes y_1, it acts on w as $S_2 w(\varphi) = w(\varphi + \theta)$ for some constant angle θ. It follows that

$$S_2 y = \cos\psi\, y_1 + \sin\psi\, w(\varphi + \theta).$$

The following proposition summarizes these observations and notations.

Proposition 12. *For points* $y \in S^2_+$ *in a neighborhood of* y_1 *we adopt spherical coordinates relative to the axis* $y_1 = \hat{\epsilon}_3$, *so that* $y = \cos\psi\,(y_1 + \tan\psi\, w(\varphi))$ *where*

$$w := w(\varphi) := \cos\varphi\,\hat{\epsilon}_1 + \sin\varphi\,\hat{\epsilon}_2.$$

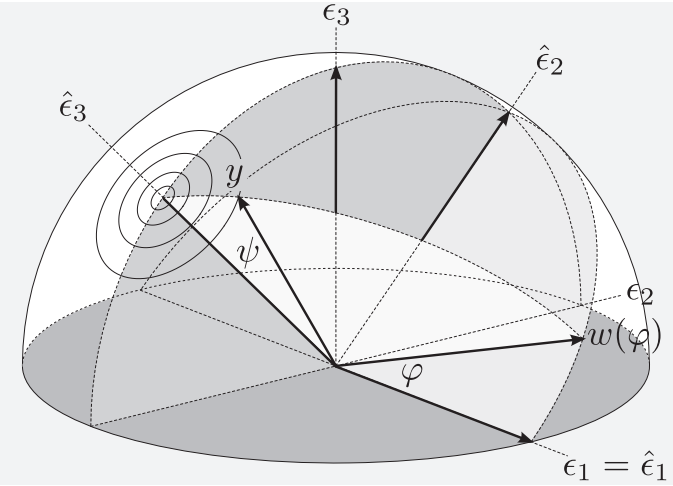

Figure 8. The velocity of orbits of the return billiard map T_2T_1, in the coordinate system Φ_1, lies in concentric circles with axis $y_1 = \hat{\epsilon}_3$. We use spherical coordinates φ and ψ relative to the axis $\hat{\epsilon}_3$ to represent the velocity $y \in S^2_+$. In these coordinates, the return map sends $w(\varphi)$ to $w(\varphi + \theta)$, where θ is a function of the wedge angle $\alpha = 2\varphi$ and the characteristic angle β of the no-slip reflection.

See figure 8. We also use the notations $[z]_3 := z \cdot \epsilon_3$, $S_1 := A_1^{-1} S A_1$, *and* $S_2 = S A_1^{-1} S A_1$. *Let* $R := T_2T_1$ *be the 2-step return map as defined above, whose domain contains a neighborhood of (x, y1) for all* $x \in \mathbb{R}^2$. *Then* $R(x, y_1) = (x, y_1)$ *for all x and*

$$R(x, y_1 + \tan\psi\, w(\varphi)) = (X, y_1 + \tan\psi\, S_2 w(\varphi)) = (X, \tan\psi\, w(\varphi + \theta))$$

for an angle θ, *depending only on the wedge angle* 2ϕ *and the characteristic angle* β *of the no-slip reflection, such that*

$$\cos\theta = (S_2\hat{\epsilon}_1) \cdot \hat{\epsilon}_1 = 1 - 8\delta^2 + 8\delta^4$$
$$\sin\theta = (S_2\hat{\epsilon}_1) \cdot \hat{\epsilon}_2 = 4\delta(1 - 2\delta^2)\sqrt{1 - \delta^2}$$

where $\delta := \cos(\beta/2)\cos\phi$. *Writing* $(X, \Phi, \Psi) = R(x, \varphi, \psi)$ *we have*

$$R : \begin{cases} X &= x + \tan\psi \frac{[A_1(x - \gamma y_1)]_3}{[y_1]_3} \frac{(I + S_1)w - \frac{[(I+S_1)w]_3 y_1}{[y_1]_3} + \tan\psi \frac{[w]_3 S_1 w - [S_1 w]_3 w}{[y_1]_3}}{1 - \tan\psi \left(\frac{[(A_1 + S_1)w]_3}{[y_1]_3} - \tan\psi \frac{[A_1 w]_3 [S_1 w]_3}{[y_1]_3^2} \right)} \\ \Phi &= \varphi + \theta \\ \Psi &= \psi \end{cases} . \quad (14)$$

Denoting $\mu_1 := \zeta_1^{-1}\epsilon_3 \in \mathbb{R}^2$, *we further have* $X(x + s\mu_1, \varphi, \psi) = X(x, \varphi, \psi) + s\mu_1$.

Since ψ remains constant under iterations of the return map $R = T_2T_1$, we regard ψ as a fixed parameter. We are interested in small values of $r := \tan\psi$. Notice that $[A_1 z]_3 := (A_1 z) \cdot \epsilon_3 = z \cdot (A_1^t \epsilon_3) = \mu_0 \cdot z$, where

$$\mu_0 := A_1^t \epsilon_3 = \begin{pmatrix} \cos(\beta/2)\sin(2\phi) \\ \sin(\beta/2)\sin(2\phi) \\ -\cos(2\phi) \end{pmatrix}.$$

Write $x_0 := \alpha y_1$, so

$$x_0 = 2\sin\phi \begin{pmatrix} 0 \\ -\sin\phi \\ \sin(\beta/2)\cos\phi \end{pmatrix}.$$

Then the proposition shows that R has the form

$$R : (x, \varphi) \mapsto (X = x + \mu_0 \cdot (x - x_0) V_r(\varphi), \Phi = \varphi + \theta) \tag{15}$$

where the vector $V_r(\varphi)$ can be made arbitrarily (uniformly) small by choosing ψ (or $r = \tan\psi$) sufficiently close to 0. Observe from the explicit form

$$V_r(\varphi) = \frac{1}{[y_1]_3} \frac{r\left((I + S_1)w - \frac{[(I+S_1)w]_3 y_1}{[y_1]_3}\right) + r^2 \frac{[w]_3 S_1 w - [S_1 w]_3 w}{[y_1]_3}}{1 - r\frac{[(A_1+S_1)w]_3}{[y_1]_3} + r^2 \frac{[A_1 w]_3 [S_1 w]_3}{[y_1]_3^2}}$$

that $V_r(\varphi) \cdot \epsilon_3 = 0$ so that X is indeed in $\mathbb{R}^2$.

Proposition 13. *The quantity* $1 + \mu_0 \cdot V_r(\varphi)$ *satisfies the coboundary relation*

$$1 + \mu_0 \cdot V_r(\varphi) = \frac{\rho(\varphi)}{\rho(\varphi + \theta)} \tag{16}$$

where

$$\rho(\varphi) = 1 + r\frac{\tan\phi}{\sin(\beta/2)}\sin\varphi.$$

In fact, the transformation R on the three-dimensional space $\mathbb{R}^2 \times \mathbb{R}/(2\pi\mathbb{Z})$*, obtained by fixing a value of* ψ *(hence of* $r = \tan\psi$*), leaves invariant the measure*

$$\mathrm{d}\mu = c\left(1 + r\frac{\tan\phi}{\sin(\beta/2)}\sin\varphi\right)\mathrm{d}A\,\mathrm{d}\varphi$$

where c is a positive constant (only dependent on the fixed parameters β, ψ, ϕ*) and A is the standard area measure on* $\mathbb{R}^2$*.*

Proof. The canonical invariant measure on $\mathbb{R}^2 \times S^2_+$ has the form $y \cdot \epsilon_3\,\mathrm{d}A\,\mathrm{d}A_S$, where A_S is the area measure on S^2_+. For a fixed value of ψ we obtain an invariant measure on $\mathbb{R}^2 \times S^1$ of the form $y \cdot \epsilon_3\,\mathrm{d}A\,\mathrm{d}\varphi$. Using the form of y given by (13), one obtains

$$y \cdot \epsilon_3 = \frac{\cos\psi\cos\phi\sin(\beta/2)}{\sqrt{1 - \cos^2(\beta/2)\cos^2\phi}}\left(1 + r\frac{\tan\phi}{\sin(\beta/2)}\sin\varphi\right).$$

This shows that, up to a multiplicative constant, the invariant measure μ has the indicated form. Equation (16) is an easy consequence of the invariance of μ with respect to R. □

By using the coordinate system $(\bar{x}, \bar{y}) \mapsto \bar{x}\mu_0 + \bar{y}\mu_1$ on $\mathbb{R}^2$, the area measure is $\mathrm{d}A = \mathrm{d}\bar{x}\,\mathrm{d}\bar{y}$ and, as observed at the end of proposition 12, the transformation R maps the fibers of the

projection $(\bar{x}, \bar{y}) \mapsto \bar{x}$ to fibers preserving the length measure on fibers. Thus we obtain a transformation $\bar{R}$ on $\mathbb{R} \times S^1$ preserving the measure $\mathrm{d}\bar{\mu}(\bar{x}, \varphi) = \rho(\varphi)\,\mathrm{d}\bar{x}\,\mathrm{d}\varphi$ where $\rho(\varphi)$ has the stated expression. Using the quotient coordinates $\bar{x} = x \cdot \mu_0$ and ϕ and writing $\overline{V}_r(\varphi) := V_r(\varphi) \cdot \mu_0$ we obtain

$$\overline{R}(\bar{x}, \phi) = \left((1 + \overline{V}_r(\varphi))\bar{x} - \bar{x}_0 \overline{V}_r(\varphi), \phi + \theta\right).$$

In particular,

$$\overline{X} = \frac{\rho(\varphi)}{\rho(\varphi + \theta)}\bar{x} + \left(1 - \frac{\rho(\varphi)}{\rho(\varphi + \theta)}\right)\bar{x}_0.$$

The invariant measure is

$$\mathrm{d}\bar{\mu}(\bar{x}, \varphi) = \rho(\varphi)\mathrm{d}\bar{x}\mathrm{d}\varphi$$

where $\rho(\varphi)$ is the density given in proposition 13. It is now immediate that

$$\overline{R}^n(\bar{x}, \varphi) = \left(\frac{\rho(\varphi)}{\rho(\varphi + n\theta)}\bar{x} + \left(1 - \frac{\rho(\varphi)}{\rho(\varphi + n\theta)}\right)\bar{x}_0, \varphi + n\theta\right).$$

This shows that all the iterates of $(\bar{x}, \varphi)$ remain uniformly close to the initial point for small values of ψ. Also notice that $(\zeta_1 \mu_0) \cdot e_{2,1} = \nu_2 \cdot e_{2,1} = \sin(2\phi) > 0$. This means that if $\bar{x}$ remains bounded, the length coordinate along the base of $\mathscr{P}_1$ also must be similarly bounded. From this we conclude:

Corollary 14. *Assume the notation introduced at the beginning of this section. For all $q \in \mathscr{P}_i \setminus (\mathscr{P}_1 \cap \mathscr{P}_2)$, $i = 1, 2$, and any neighborhood $\mathscr{V}$ of the period-2 state $(q, v_i) \in S_i^+$, there exists a small enough neighborhood $\mathscr{U} \subset \mathscr{V}$ of (q, v_i) the orbits of whose points remain in $\mathscr{V}$.*

The following theorem is now immediate.

Theorem 15. *Polygonal no-slip billiards having a corner of inner angle less than π cannot be ergodic for the canonical invariant measure.*

7. Higher order periodic orbits in polygons

The analysis of the previous section is based on the existence of period-2 orbits in wedge-shaped no-slip billiard tables. Existence of periodic orbits of higher periods presently seems difficult to establish analytically, although one such result for wedge domains will be indicated below in this section, which strengthens an observation made in [4]. We first point out a generalization of corollary 14 to perturbations of periodic orbits in general polygon-shaped domains.

Figure 9 illustrates the type of stability implied by the following theorem 16.

Theorem 16. *Periodic orbits in no-slip polygon-shaped billiard domains are Lyapunov stable. That is, given an initial state $\xi_0 = (q_0, v_0)$ for a period-n orbit in such a billiard system, and for any neighborhood $\mathscr{V}$ of ξ_0, there exists a small enough neighborhood $\mathscr{U} \subset \mathscr{V}$ of ξ the orbits of whose elements remain in $\mathscr{V}$.*

Proof. The idea is essentially the same as used in the proof of proposition 13 and corollary 14. We only indicate the outline. By a choice of convenient coordinates around the periodic

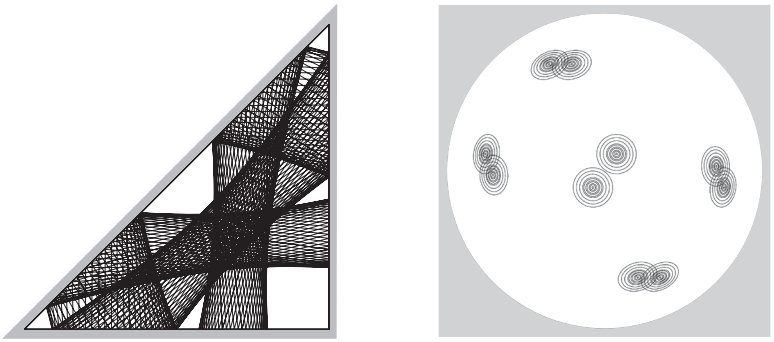

Figure 9. Theorem 16 states that periodic orbits of polygonal billiards are Lyapunov stable. This is illustrated here by a period-10 orbit of a triangular no-slip billiard. The right-hand side shows projections to the velocity phase space of several orbits near the one of period-10. (The projection of the periodic orbit consists of the 10 centers of the family of concentric circles.) One of the neighboring orbits is also shown on the left-hand side, projected to the plane of the billiard table.

point, it is possible to show that the nth iterate of the billiard map T, denoted $R := T^n$, can be regarded as a map from an open subset of $\mathbb{R}^2 \times S^1$ into this latter set, having the form $R(x,\varphi) = (x_0 + A(\varphi)(x - x_0), \varphi + \theta)$ for a certain angle θ, where $A(\varphi)$ is a linear transformation independent of x. Rotation invariance implies that R must satisfy the invariance property $R(x + su, \varphi) = R(x,\varphi) + su$ for a vector $u \in \mathbb{R}^2$. From this we define a map $\overline{R}$ on (a subset of) the quotient $\mathbb{R} \times S^1$, $\mathbb{R}^2/\mathbb{R}u$ being identified with $\mathbb{R}$. Furthermore, denoting by $(\bar{x}, \varphi)$ the coordinates in this quotient space, invariance of the canonical measure implies invariance of a measure μ on this quotient having the form $\mathrm{d}\mu(\bar{x},\varphi) = \rho(\varphi)\,\mathrm{d}\bar{x}\,\mathrm{d}\varphi$. Invariance is with respect to the quotient map $\overline{R}(\bar{x},\varphi) = (\bar{x}_0 + a(\varphi)(\bar{x} - \bar{x}_0), \varphi + \theta)$ for some function $a(\varphi)$. This function must then take the form $a(\varphi) = \rho(\varphi)/\rho(\varphi + \theta)$. Iterates of $\overline{R}$ will then behave like the corresponding map for the wedge domain, defined prior to theorem 14. □

We briefly turn our attention here to the question of existence of periodic orbits of higher (necessarily even) periods for wedge shapes. Clearly, a necessary condition for periodicity is that the angle θ introduced in proposition 12 (see also figure 8) be rational. For orbits that do not eventually escape to infinity, this is also a sufficient condition, as a simple application of Poincaré recurrence shows. (See [4].) Moreover, as θ is only a function of $\delta := \cos(\beta/2)\cos\phi$, which is given by (proposition 12)

$$\cos\theta = 1 - 8\delta^2 + 8\delta^4 \tag{17}$$

where β is the characteristic angle of the system (a function of the mass distribution on the disc) and 2ϕ is the corner angle of the wedge domain, if a higher order periodic orbit exists for a given δ, all bounded orbits have the same period.

Consider now the case of uniform mass distribution, for which $\cos(\beta/2) = \sqrt{2/3}$. Solving (17) for $\cos\phi$, for $\theta = 2\pi p/q$, choosing first the negative square root, gives

$$\cos\phi_{p,q} := \frac{\sqrt{3}}{2}\sqrt{1 - \sqrt{\frac{1 + \cos(2\pi p/q)}{2}}}. \tag{18}$$

Notice that there are no restrictions on the values of p and q. The following proposition is a consequence of these remarks.

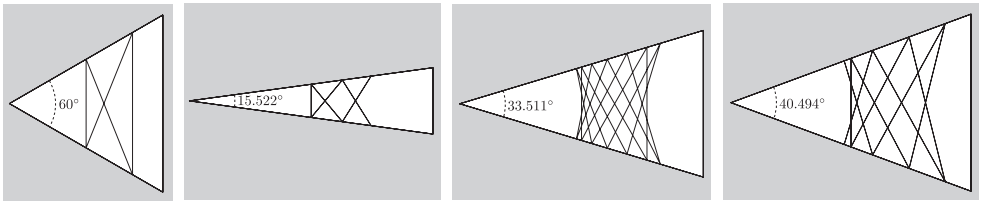

Figure 10. From left to right: projections of periodic orbits of periods $4, 10, 14, 18$. (Bounded orbits in the same wedge domain are all periodic with the same period.) The rotation angle θ in each case is $2\pi p/q$ where p/q is $1/2, 2/5, 3/7, 4/9$, respectively. Mass distribution is uniform.

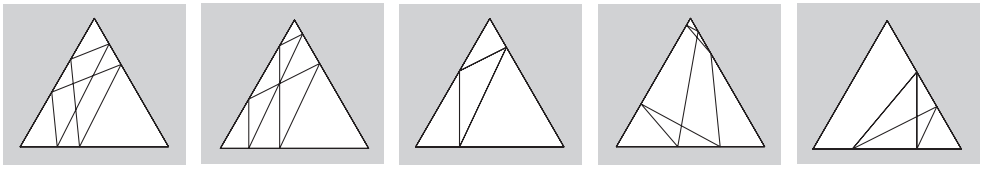

Figure 11. All orbits of an equilateral triangle no-slip billiard system are periodic with (not necessarily least) period equal to four or six.

Theorem 17. *For any positive even integer n there exists a wedge domain for which the no-slip billiard has period-n orbits. More specifically, all bounded orbits of the no-slip billiard in a wedge domain with corner angle $\phi_{p,q}$ satisfying equation 18 are periodic with period $2q$.*

Solving 17 for $\cos\phi$, for $\theta = 2\pi p/q$, but choosing now the positive square root, gives

$$\cos\phi_{p,q} := \frac{\sqrt{3}}{2}\sqrt{1+\sqrt{\frac{1+\cos(2\pi p/q)}{2}}}.$$

This makes sense so long as $0.392 \approx \arccos(-7/9)/2\pi \leqslant p/q \leqslant 0.5$, which greatly restricts the choices of p and q. A few examples in this case are shown in figure 10.

It is interesting to observe that all orbits of the equilateral triangle are periodic with period four or six. (See figure 11 and [4] for the proof.) We do not know of any other no-slip billard domain all of whose orbits are periodic.

8. Linear stability in the presence of curvature

We now turn to the problem of characterizing stability of period-2 orbits for no-slip billiard domains whose boundary may have non-zero geodesic curvature. Here we only address *linear* rather than local stability. In other words, we limit ourselves to the problem of determining when the differential of the billiard map at a period-2 collision state $\xi = (q, v)$ is elliptic or hyperbolic, and obtaining sharp thresholds (where it is parabolic). A simple but key observation is contained in the following lemma.

Lemma 18. *Let $\xi = (q, v)$ be periodic with period 2 for the no-slip billiard map and consider the differential $\mathscr{T} := \mathrm{d}T^2_\xi : v^\perp \oplus v^\perp \to v^\perp \oplus v^\perp$. Then either all the eigenvalues of $\mathscr{T}$ are real, of the form $1, 1, r, 1/r$ or, if not all real, they are $1, 1, \lambda, \overline{\lambda}$ where $|\lambda| = 1$.*

Proof. This is a consequence of the following observations. First, we know that $T^*\Omega = -\Omega$, where Ω is the canonical volume form (see section 5). Therefore, the product of the eigenvalues of $\mathscr{T}$ counted with multiplicity is 1. The vector (e_1, w_1), where e_1 is the first vector in the product frame and w_1 is the first vector in the wavefront frame, is an eigenvector for eigenvalue 1 of $\mathrm{d}T_\xi$ due to rotation symmetry, as already noted. If we regard $\mathrm{d}T_\xi$ as a self-map of $v^\perp \oplus v^\perp$ as in the corollary to proposition 7 then we should use instead the vector (w_1, w_1). (Recall that w_1 is collinear with the orthogonal projection of e_1 to $v^\perp$.) In addition, by reversibility of T, if λ is an eigenvalue of $\mathscr{T}$, then $1/\lambda$ also is, and since $\mathscr{T}$ is a real valued linear map, the complex conjugates $\overline{\lambda}$ and $1/\overline{\lambda}$ are also eigenvalues. As the dimension of the linear space is 4, if one of the eigenvalues, λ, is not real, it must be the case that $\lambda = 1/\overline{\lambda}$ and we are reduced to the case $1, 1, \lambda, \overline{\lambda}$ with $\lambda\overline{\lambda} = 1$. If all eigenvalues are real, and $r \neq 1$ is an eigenvalue, then we are reduced to the case $1, 1, r, 1/r$. □

Corollary 19. *The period-2 point ξ is elliptic for $\mathscr{T} = \mathrm{d}T_\xi^2$ if and only if $|Tr(\mathscr{T}) - 2| < 2$.*

To proceed, it is useful to express the differential map of corollary 8 in somewhat different form. First observe, in the period-2 case (in which $\tilde{v} = -v$ and $v^\perp = \tilde{v}^\perp$), that

$$w_2(\xi) = -w_2(\tilde{\xi}) \text{ and } \frac{\cos\psi(\tilde{q}, v)}{\cos\phi(\tilde{q}, v)} = \frac{\cos\psi(\tilde{\xi})}{\cos\phi(\tilde{\xi})} = \frac{\cos\psi(\xi)}{\cos\phi(\xi)}.$$

(See section 3.) Now define the rank-1 operator

$$\Theta_{\tilde{\xi}}(Z) := 2\cos(\beta/2)\frac{\cos\psi(\tilde{\xi})}{\cos\phi(\tilde{\xi})}\left\langle w_2(\tilde{\xi}), Z\right\rangle u_1(\tilde{q}).$$

Then

$$\mathrm{d}T_\xi \begin{pmatrix} X \\ Y \end{pmatrix} = \begin{pmatrix} I & tI \\ -\kappa(\tilde{q})\Theta_{\tilde{\xi}} & C_{\tilde{q}} - t\kappa(\tilde{q})\Theta_{\tilde{\xi}} \end{pmatrix} \begin{pmatrix} X \\ Y \end{pmatrix}. \tag{19}$$

When $\kappa(q) = \kappa(\tilde{q})$ there is a simplification in the criterion for ellipticity, as will be seen shortly. With this special case in mind we define the linear map R_ξ on $v^\perp$ by $R_\xi w_i(\xi) = -(-1)^i w_i(\xi)$, $i = 1, 2$. Notice that $Ru_1(q) = u_1(\tilde{q})$. Then

$$R_{\tilde{\xi}} C_{\tilde{q}} = C_q R_\xi, \quad R_{\tilde{x}}\Theta_{\tilde{\xi}} = \Theta_\xi R_\xi.$$

The same notation R_ξ will be used for the map on $v^\perp \oplus v^\perp$ given by $(z_1, z_2) \mapsto (R_\xi z_1, R_\xi z_2)$. Then $R := R_\xi = R_{\tilde{\xi}}$ since $w_i(\tilde{\xi}) = -(-1)^i w_i(\xi)$. It follows that

$$R\mathrm{d}T_\xi R = \begin{pmatrix} I & tI \\ -\kappa(\tilde{q})\Theta_\xi & C_q - t\kappa(\tilde{q})\Theta_\xi \end{pmatrix}. \tag{20}$$

In particular, when $\kappa(q) = \kappa(\tilde{q})$, we have $R\mathrm{d}T_\xi R = \mathrm{d}T_{\tilde{\xi}}$ and $\mathrm{d}T_{\tilde{\xi}}^2 = (R\mathrm{d}T_\xi)^2$. Therefore, rather than computing the trace of $\mathrm{d}T_{\tilde{\xi}}^2$, we need only consider the easier to compute trace of RdT_ξ. The result is recorded in the next lemma.

Lemma 20. *Let $\xi = (q, v)$ have period 2 and set $\tilde{\xi} := T(\xi)$, $C := C_q, \Theta := \Theta_q$. Then*

$$Tr\left(\mathrm{d}T_{\tilde{\xi}}^2\right) = Tr\left\{I + (CR)^2 - t(\kappa(q) + \kappa(\tilde{q}))\left[\Theta + (CR)(\Theta R)\right] + t^2\kappa(q)\kappa(\tilde{q})(\Theta R)^2\right\}.$$

When $\kappa := \kappa(\tilde{q}) = \kappa(q)$, we have $Tr(R\mathrm{d}T_\xi) = Tr\left(CR + t\kappa\Theta\right)$.

Proof. These expressions follow easily given the above definitions and notations. □

The traces can now be computed using Equations (3) and (4). The matrices expressing C, R, Θ in the wavefront basis of $v^{\perp}$ are given as follows. For convenience we write

$$c := \cos(\beta/2),\ c_\phi := \cos\phi,\ c_\psi := \cos\psi,\ \varrho := \sqrt{1-\cos^2(\beta/2)\cos^2\phi},$$

where $\phi = \phi(\xi)$ and $\psi = \psi(\xi)$ are defined in corollary 8.

$$[C]_w = \begin{pmatrix} 1-2c^2c_\phi^2 & -2cc_\phi\varrho \\ -2cc_\phi\varrho & -1+2c^2c_\phi^2 \end{pmatrix},\ [R] = \begin{pmatrix} 1 & 0 \\ 0 & -1 \end{pmatrix},\ [\Theta]_w = 2c\frac{c_\psi}{c_\phi}\begin{pmatrix} 0 & \varrho \\ 0 & -cc_\phi \end{pmatrix}.$$

Let $\bar{d}$ be the distance between the projections of q and $\tilde{q}$ on plane the billiard table, $\overline{v}$ the projection of v on the same plane and t, as before, the time between consecutive collisions. From $\cos\psi = \sin(\beta/2)\cos\phi/\sqrt{1-\cos^2(\beta)\cos^2\phi}$ it follows that $t\cos\psi = \cos\phi\,\bar{d}$.

We then obtain

$$\mathrm{Tr}\,(RdT_\xi) = \mathrm{Tr}(CR) + t\kappa\mathrm{Tr}(\Theta) = 2\left[1-2\cos^2(\beta/2)\cos^2\phi\right] - 2\kappa\bar{d}\cos^2(\beta/2)\cos\phi \tag{21}$$

and

$$\begin{aligned}\mathrm{Tr}\left(\mathrm{d}T_\xi^2\right) = 4\Big\{&\left[1-2\cos^2(\beta/2)\cos^2\phi\right]^2 \\ &-(\kappa(q)+\kappa(\tilde{q}))\cos^2(\beta/2)\cos\phi\left[1-2\cos^2(\beta/2)\cos^2\phi\right]\bar{d} \\ &+\kappa(q)\kappa(\tilde{q})\cos^4(\beta/2)\cos^2\phi\,\bar{d}^2\Big\}.\end{aligned} \tag{22}$$

Observe that in the special case in which $\kappa(q) = \kappa(\tilde{q})$ we have

$$\mathrm{Tr}\left(\mathrm{d}T_\xi^2\right) = \left\{2\left[1-2\cos^2(\beta/2)\cos^2\phi\right] - 2\kappa\cos^2(\beta/2)\cos\phi\,\bar{d}\right\}^2.$$

Theorem 21. *Suppose that the billiard domain has a piecewise smooth boundary with at least one corner having inner angle less than π. Then, arbitrarily close to that corner point, the no-slip billiard has (linearly) elliptic period-2 orbits.*

Proof. Period-2 orbits exist arbitrarily close to the corners of a piecewise smooth billiard domain as figure 12 makes clear. For period-2 orbits near a corner the above expression for $\mathrm{Tr}\left(\mathrm{d}T_\xi^2\right)$ gives for small $\bar{d}$

$$0 < \mathrm{Tr}\left(\mathrm{d}T_\xi^2\right) = 4\left[1-2\cos^2(\beta/2)\cos^2\phi\right]^2 + O(\bar{d}) < 4.$$

This implies that

$$\left|\mathrm{Tr}\left(\mathrm{d}T_\xi^2\right) - 2\right| < 2$$

and the theorem follows from corollary 19. □

Let us consider the special case of equal curvatures at q and $\tilde{q}$. Define $\zeta := \kappa\bar{d}$. When $\zeta > 0$ (equivalently, the curvature is positive), the critical value of ζ is

$$\zeta_0 = \frac{2-2\cos^2(\beta/2)\cos^2\phi}{\cos^2(\beta/2)\cos\phi}. \tag{23}$$

The condition for ellipticity is $\zeta > \zeta_0$. When $\zeta < 0$, the critical value of ζ is

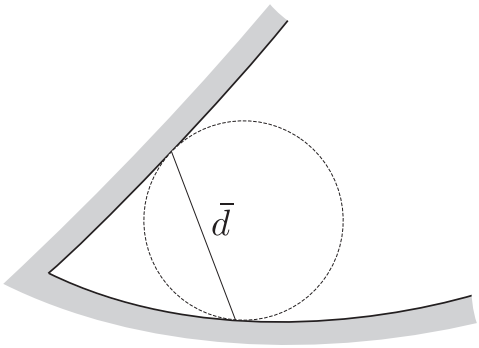

Figure 12. For a billiard domain with piecewise smooth boundary, arbitrarily near any corner with inner angle less than π there are linearly stable period-2 orbits.

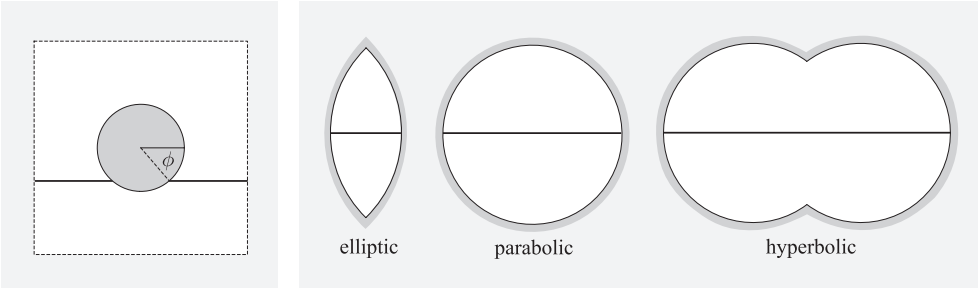

Figure 13. Two families of periodic orbits. On the left: the no-slip Sinai billiard and a period-2 orbit whose projection to the plane of the billiard domain hits the circular scatterer at an angle ϕ. On the right: a family of billiard domains with negative boundary curvature; the period-2 orbits project to the thick horizontal lines.

$$\zeta_0 = -2\cos\phi$$

and the condition for ellipticity is $|\zeta| < |\zeta_0|$.

Theorem 21 together with numerical experiments strongly suggests that such no-slip billiards will aways admit small invariant open sets and thus cannot be ergodic with respect to the canonical billiard measure.

9. Two numerical examples

We now illustrate the curvature cut-off in two numerical examples corresponding to the two families of periodic orbits shown in figure 13. On the left-hand side of the figure is the no-slip version of the Sinai billiard. (We refer to [12] for more information and motivation about this system. That paper explains how it models the motion of two discs in a torus with no-slip contact.) The billiard domain is the complement of a circular scatterer in a two-torus.

We focus attention on a family of horizontal period-2 orbits parametrized by the angle ϕ shown in the figure. As already remarked, the actual configuration manifold is the 3-dimensional space M that includes the angle of rotation of the moving disc; for the no-slip Sinai billiard, this three-dimensional space, and the same periodic orbit we consider now, were already shown in figure 6. (The symbol ϕ in that figure plays the same role as in the

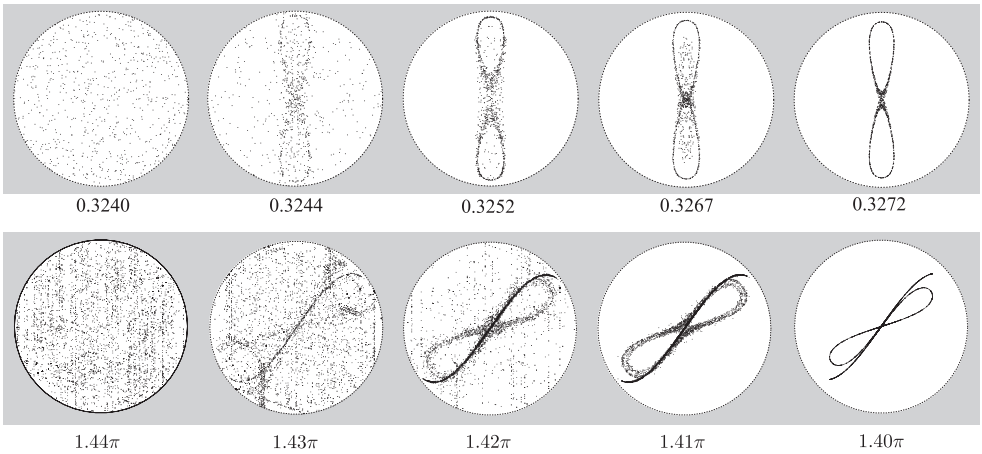

Figure 14. Top row: velocity phase portraits of a single orbit near the periodic orbit of the no-slip Sinai billiard corresponding to $\phi = 0$. The radius of the circular scatterer is given under each portrait. Bottom row: similarly for an orbit near the periodic one given in the right-hand part of figure 13. The numbers are the circular cap angles (so π corresponds to the disc domain in figure 13.) Apparent chaotic behavior occurs for an angle much greater than π. This is expected since period-2 orbits parallel to the one at middle height, but not too far from it, remain linearly stable for larger angle cap values.

present discussion.) See also figure 9, which may help to interpret the below figure 14. Note that such a periodic orbit exists for ϕ arbitrarily close to $\pi/2$. In [12] only the orbit for $\phi = 0$ was considered.

On the right-hand side of figure 13 is a family of billiard domains whose boundary consists in each case of a pair of circular arcs. This family of examples is parametrized by the angle of the arcs. Here we only consider the horizontal period-2 orbit through the center of these domains. Thus these two classes of systems would correspond to the so-called dispersing and the focusing billiards if we were dealing with the ordinary type of collision. In all cases, the mass distribution of the moving disc is uniform.

We first examine small perturbations of the periodic orbit in the no-slip Sinai billiard system corresponding to $\phi = 0$. The critical radius of the circular scatterer, which can be obtained from equation (23), is exactly 1/3. This was already shown in [12].

The top row of figure 14 suggests a transition from chaotic to more regular type of behavior for a radius between 0.32–0.33. So the observed numbers are somewhat smaller than the exact value 1/3. We should bear in mind that the periodic points are not isolated, but are part of the family parametrized by ϕ. As ϕ increases, the critical parameter ζ_0 changes (for the uniform mass distribution, where $\cos^2(\beta/2) = 2/3$) according to the expression $\zeta_0 = (3 - \cos^2\phi)/\cos\phi$. Given in terms of the radius of curvature, $\zeta = (1 - 2R\cos\phi)/R$. Solving for the critical R yields $R_0 = \frac{\cos\phi}{3}$. Thus for a period-2 trajectory having a small but non-zero ϕ, the critical radius is less than 1/3. It is then to be expected that the experimental critical value of R, for orbits closed to that having $\phi = 0$ will give numbers close to but less than 1/3. Moreover, as R_0 approaches 0 when ϕ approaches $\pi/2$, we obtain the following proposition which, together with experimental evidence indicates that the no-slip Sinai billiard is never ergodic no matter how small the value of the scatterer's radius. This phenomenon is further illustrated in figure 15.

Proposition 22. *The no-slip Sinai billiard, for any choice of scatterer curvature, will con-*

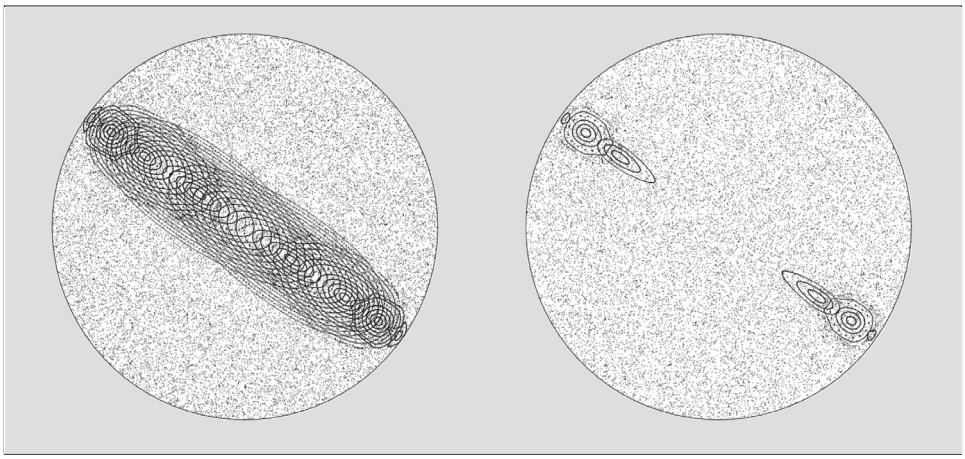

Figure 15. On the left: velocity phase portrait of the no-slip Sinai billiard with scatterer radius $R = 0.35$. Since this is greater than the transition value $R = 1/3$, the period-2 orbits parametrized by ϕ are all elliptic. On the right, $R = 0.32$ and ellipticity has been destroyed for orbits with smaller values of ϕ. No matter how small R is, elliptic orbits always exist for ϕ sufficiently close to $\pi/2$.

tain (linearly) elliptic periodic trajectories of period 2.

As another example, consider the family of billiard regions bounded by two symmetric arcs of circle depicted in figure 13. In this case, the critical transition from hyperbolic to elliptic, for the horizontal periodic orbit at middle height shown in the figure, happens for the disc domain. This is again shown using equation (23).

Numerically, a transition similar to that observed for the Sinai billiard is seen to occur near the horizontal period-2 orbit passing through the center of the billiard domain. The number indicated below each velocity phase portrait in the bottom row of figure 14 is the angle of the circular arc. Thus, for example, the disc corresponds to angle π while smaller angles give the lemon shaped domains. Hence the exact cut-off angle at which the indicated periodic orbit becomes elliptic is π. Notice, however, that the experimental value for this angle is greater than π. Just as in the Sinai billiard example, we should keep in mind that the periodic orbits are not isolated; while ellipticity is destroyed for the middle height orbit, others parallel to it may still be elliptic. Here the bias is towards greater values of the angle. In other words, the structures we see in the velocity phase portrait are associated to periodic orbits near the one at middle height, and for them the cut-off angle of the circular arcs is greater than π.

10. Final remark

Of the results discussed above, the more complete ones apply to polygonal no-slip billiards; they imply a strong stability of periodic orbits. For general curvature, we also noted above that elliptic behavior is very common and hard to destroy.

A general picture for polygonal billiards emerges from the numerical examples, which we cannot yet validate analytically: it appears that all orbits (in an open invariant set of full measure) lie in a stable neighborhood of some periodic orbit. In other words, what is shown in figure 9 is what all orbits look like in numerical experiments: those that are not periodic all seem to lie in an elliptic island of a periodic orbit. On the other hand, in the presence of

boundary curvature, stable and chaotic dynamics seem to coexist in all examples considered so far. In particular, finding an example of ergodic no-slip billiard system (relative to the Liouville measure in the reduced three-dimensional phase space) seems to be a challenging problem at the moment.

Acknowledgments

H-KZ was partially supported by NSF grant DMS-1151762 and a grant from the Simons Foundation (337646, HZ).

References

[1] Broomhead D S and Gutkin E 1993 The dynamics of billiards with no-slip collisions *Physica* D **67** 188–97
[2] Chernov N and Markarian R 2006 *Chaotic Billiards* (*Mathematical Surveys and Monographs* vol 127) (Providence, RI: American Mathematical Society)
[3] Cox C and Feres R 2016 Differential geometry of rigid bodies collisions and non-standard billiards *Discrete Continuous Dyn. Syst.* A **36** 6065–99
[4] Cox C and Feres R 2017 No-slip billiards in dimension two *Dynamical Systems, Ergodic Theory, and Probability: in Memory of Chernov* (*Contemporary Mathematics* vol 698) (Providence, RI: American Mathematical Society) pp 91–110 (https://doi.org/10.1090/conm/698/14032)
[5] Garwin R L 1969 Kinematics of an ultraelastic rough ball *Am. J. Phys.* **37** 88–92
[6] Kaloshin V, Mather J N and Valdinoci E 2004 Instability of Resonant Totally Elliptic Points of Symplectic Maps in Dimension 4. Analyse complexe, systèmes dynamiques, sommabilité des séries divergentes et théories galoisiennes. II *Astérisque* **297** 79–116
[7] Larralde H, Leyvraz F and Mejía-Monasterio C 2003 Transport properties of a modified Lorentz gas *J. Stat. Phys.* **113** 197–231
[8] Moser J 1962 On invariant curves of area-preserving mappings of an annulus *Nachr. Akad. Wiss. Göttngen* **II** 1–20
[9] Mejía-Monasterio C, Larralde H and Leyvraz F 2001 Coupled normal heat and matter transport in a simple model system *Phys. Rev. Lett.* **86** 5417–20
[10] Sevryuk M B 1986 *Reversible Systems* (*Lecture Notes in Mathematics 1211*) (Berlin: Springer)
[11] Sevryuk M B 1991 Lower dimensional Tori in reversible systems *Chaos* **1** 160–7
[12] Wojtkowski M 1994 The system of two spinning disks in the torus *Physica* D **71** 430–9